8/3/05

# Gene Set Enrichment Analysis: A Knowledge-Based Approach for Interpreting Genome-wide Expression Profiles

**Aravind Subramanian[*,†], Pablo Tamayo[*,†], Vamsi K. Mootha[†,‡], Sayan Mukherjee[§], Benjamin L. Ebert[†,¶], Michael A. Gillette[†,‖], Amanda Paulovich[¶¶], Scott L. Pomeroy[**], Todd R. Golub[†,¶], Eric S. Lander[†,‡,††,‡‡], Jill P. Mesirov[†]**

* These authors contributed equally to this work

† Broad Institute of MIT and Harvard, 320 Charles St. Cambridge, MA, 20141

‡ Department of Systems Biology, Alpert 536, Harvard Medical School, 200 Longwood Ave, Boston, MA 02446

§ Institute for Genome Sciences and Policy, CIEMAS, Duke University
101 Science Drive, Durham, NC 27708

¶ Department of Medical Oncology, Dana-Farber Cancer Institute, 44 Binney Street, Boston, MA 02115

‖ Division of Pulmonary and Critical Care Medicine, Massachusetts General Hospital, 55 Fruit Street, Boston, MA 02114

¶¶Fred Hutchinson Cancer Research Center, 1100 Fairview Avenue N., C2-023
PO Box 19024, Seattle, WA 98109-1024

**Department of Neurology, Enders 260, Children's Hospital, Harvard Medical School, 300 Longwood Avenue, Boston, MA 02115

†† Department of Biology, Massachusetts Institute of Technology, Cambridge, Massachusetts 02142

‡‡ Whitehead Institute for Biomedical Research, Massachusetts Institute of Technology, Cambridge, Massachusetts 02142

Classification: Biological Sciences; Genetics

Correspondence should be addressed to:
Jill P. Mesirov
Broad Institute of MIT and Harvard
Cambridge, MA 02141
Phone: (617) 252-1919, Fax: (617) 252-1933
E-mail: mesirov@broad.mit.edu

Abbreviations: FDR, GSEA, MHT, MSigDB

**Abstract**

Although genome-wide RNA expression analysis has become a routine tool in biomedical research, extracting biological insight from such information remains a major challenge. Here, we describe a powerful analytical method called Gene Set Enrichment Analysis (GSEA) for interpreting gene expression data. The method derives its power by focusing on *gene sets* – that is, groups of genes that share common biological function, chromosomal location or regulation. We demonstrate how GSEA yields insights into several cancer-related datasets, including leukemia and lung cancer. Notably, where single-gene analysis finds little similarity between two independent studies of patient survival in lung cancer, GSEA reveals many biological pathways in common.
The GSEA method is embodied in a freely available software package, together with an initial database of 1325 biologically defined gene sets.

## 1. Introduction

Genome-wide expression analysis using DNA microarrays has become a mainstay of genomics research (1, 2). The challenge no longer lies in *obtaining* gene expression profiles, but rather in *interpreting* the results to gain insights into biological mechanisms.

In a typical experiment, mRNA expression profiles are generated for thousands of genes from a collection of samples belonging to one of two classes—for example, tumors that are sensitive vs. resistant to a drug. The genes can be ordered in a ranked list $L$, according to their differential expression between the classes. The challenge is to extract meaning from this list.

A common approach involves focusing on a handful of genes at the top and bottom of $L$ (i.e., those showing the largest difference), to discern telltale biological clues. This approach has a few major limitations:

(i) After correcting for multiple hypotheses testing (MHT), no individual gene may meet the threshold for statistical significance, because the relevant biological differences are modest relative to the noise inherent to the microarray technology.

(ii) Alternatively, one may be left with a long list of statistically significant genes without any unifying biological theme. Interpretation can be daunting and *ad hoc,* being dependent on a biologist's area of expertise.

(iii) Single-gene analysis may miss important effects on pathways. Cellular processes often affect *sets* of genes acting in concert. An increase of 20% in all genes encoding members of a metabolic pathway may dramatically alter the flux through the pathway and may be more important than a 20-fold increase in a single gene.

(iv) When different groups study the same biological system, the list of statistically significant genes from the two studies may show distressingly little overlap (3).

To overcome these analytical challenges, we recently developed a method called Gene Set Enrichment Analysis (GSEA) that evaluates microarray data at the level of *gene sets*. The gene sets are defined based on prior biological knowledge, *e.g.,* published information about biochemical pathways or co-expression in previous experiments. The goal of GSEA is to determine whether members of a gene set *S* tend to occur toward the top (or bottom) of the list *L*, in which case the gene set is correlated with the phenotypic class distinction.

We used a preliminary version of GSEA to analyze data from muscle biopsies from diabetics vs. healthy controls (4). The method revealed that genes involved in oxidative phosphorylation (OXPHOS) show reduced expression in diabetics, although the average decrease per gene is only 20%. The results from this study have been independently validated by other microarray studies (5) and by *in vivo* functional studies (6).

Given this success, we have developed GSEA into a robust technique for analyzing molecular profiling data. We studied its characteristics and performance and substantially revised and generalized the original method for broader applicability.

In this paper, we provide a full mathematical description of the GSEA methodology and illustrate its utility by applying it to several diverse biological problems. We have also created a software package, called GSEA-P and an initial inventory of gene sets (MSigDB), both of which are freely available.

## 2. Overview of GSEA

GSEA considers experiments with genome-wide expression profiles from samples belonging to two classes, labeled 1 or 2. Genes are ranked based on the correlation between their expression and the class distinction, using any suitable metric (Fig. 1A).

Given an a priori defined set of genes *S* (e.g., genes encoding products in a metabolic pathway, located in the same cytogenetic band, or sharing the same GO category), the goal of GSEA is to determine whether the members of *S* are randomly distributed throughout *L*, or primarily found at the top or bottom. We expect that sets related to the phenotypic distinction will tend to show the latter distribution.

There are three key elements of the GSEA method:

**Step 1: Calculation of an enrichment score.** We calculate an enrichment score (*ES*) that reflects the degree to which a set *S* is over-represented at the extremes (top or bottom) of the entire ranked list *L*. The score is calculated by walking down the list *L*, increasing a running-sum statistic when we encounter a gene in *S* and decreasing it when we encounter genes not in *S*. The magnitude of the increment depends on the correlation of the gene with the phenotype. The enrichment score is the maximum deviation from zero encountered in the random walk; it corresponds to a weighted Kolmogorov-Smirnov-like statistic (7) (Fig. 1B).

**Step 2: Estimation of significance level of *ES*.** We estimate the statistical significance (nominal *P*-value) of the *ES,* using an empirical phenotype-based permutation test procedure that preserves the complex correlation structure of the gene expression data. Specifically, we permute the phenotype labels and re-compute the *ES* of the gene set for the permutated data; this generates a null distribution for the *ES*. The empirical, nominal *P*-value of the observed *ES* is then calculated relative to this null distribution. Importantly, the permutation of class labels preserves gene-gene correlations and thus provides a more biologically reasonable assessment of significance than would be obtained by permuting genes.

**Step 3: Adjustment for multiple hypothesis testing.** When an entire database of gene sets is evaluated, we adjust the estimated significance level to account for multiple hypothesis testing (MHT). We first normalize the *ES* for each gene set to account for the size of the set, yielding a normalized enrichment score (*NES)*. We then control the

proportion of false positives by calculating the false discovery rate (FDR) (8, 9) corresponding to each *NES*. The FDR is the estimated probability that a set with a given *NES* represents a false positive finding; it is computed by comparing the tails of the observed and null distributions for the *NES*.

The details of the implementation are described in the Appendix and Supporting Information.

We note that the GSEA method differs in several important ways from the preliminary version (see Supporting Information). In the original implementation, the running-sum statistic used equal weights at every step. However, we found that this yielded high scores for sets clustered near the middle of the ranked list (Fig. 2A); these sets do not represent biologically-relevant correlation with the phenotype. We addressed this by weighting the steps according to each gene's correlation with phenotype. We noticed that the use of weighted steps could cause the distribution of observed *ES* scores to be asymmetric in cases where many more genes are correlated with one of the two phenotypes. We therefore estimate the significance levels by considering separately the positively- and negatively-scoring gene sets (see Appendix and Supporting Information Fig. SF1).

Our preliminary implementation used a different approach, family-wise-error rate (FWER), to correct for MHT. The FWER is a conservative correction that seeks to ensure that the list of reported results does not include even a single false-positive gene set. This criterion turned out to be so conservative that many applications yielded no statistically significant results. Because our primary goal is to generate hypotheses, we chose to use the FDR to focus on controlling the probability that each reported result is a false positive.

Based on our statistical analysis and empirical evaluation, GSEA shows broad applicability. It can detect subtle enrichment signals and it preserves our original results in (4), with the OXPHOS pathway significantly enriched in the normal samples ($P$ = .008, $FDR$ = .04). This methodology has been implemented in a software tool called GSEA-P.

**3. The leading-edge subset**

Gene sets can be defined using a variety of methods, but not all the members of a gene set will typically participate in a biological process. Often it is useful to extract the core members of high scoring gene sets that contribute to the *ES*. We define the *leading-edge subset* to be those genes in the gene set *S* that appear in the ranked list *L* at, or before, the point where the running sum reaches its maximum deviation from zero (Fig. 1B). The leading-edge subset can be interpreted as the core of a gene set that accounts for the enrichment signal.

Examination of the leading-edge subset can reveal a biologically important subset within a gene set as we show below in our analysis of P53 status in cancer cell lines. This is especially useful with manually curated gene sets, which may represent an amalgamation of interacting processes. We first observed this in our previous study (4) where we manually identified two high scoring sets, a curated pathway and a computationally derived cluster, which shared a large subset of genes later confirmed to be a key regulon altered in human diabetes.

High scoring gene sets can be grouped on the basis of leading-edge subsets of genes that they share. Such groupings can reveal which of those gene sets correspond to the same biological processes and which represent distinct processes.

The GSEA-P software package includes tools for examining and clustering leading-edge subsets (Supporting Information).

**4. An initial catalog of human gene sets**

GSEA evaluates a query microarray dataset using a collection of gene sets. We therefore created an initial catalog of 1325 gene sets, which we call the Molecular Signature Database (MSigDB 1.0) (Table S1 and Supporting Information), consisting of four types of sets:

**Cytogenetic sets ($C_1$, 319 gene sets)**. This catalog includes 24 sets, one for each of the 24 human chromosomes, and 295 sets corresponding to cytogenetic bands. These sets are helpful in identifying effects related to chromosomal deletions or amplifications, dosage compensation, epigenetic silencing and other regional effects.

**Functional sets ($C_2$, 522 gene sets).** This catalog includes 472 sets containing genes whose products are involved in specific metabolic and signaling pathways, as reported in

eight publicly available, manually curated databases, and 50 sets containing genes co-regulated in response to genetic and chemical perturbations, as reported in various experimental papers.

**Regulatory-motif sets ($C_3$, 57 gene sets).** This catalog is based on our recent work reporting 57 commonly conserved regulatory motifs in the promoter regions of human genes (10), and makes it possible to link changes in a microarray experiment to a conserved, putative *cis*-regulatory element.

**Neighborhood sets ($C_4$, 427 gene sets).** This catalog consists of sets defined by expression neighborhoods centered on cancer-related genes.

This database provides an initial collection of gene sets for use with GSEA and illustrates the types of gene sets that can be defined, including those based on prior knowledge or derived computationally.

## 5. Applications of GSEA

We explored the ability of GSEA to provide biologically meaningful insights in six examples for which considerable background information is available.

In each case, we searched for significantly associated gene sets from one or both of the subcatalogs $C_1$ and $C_2$ - above. Table 1 lists all gene sets with an FDR $\leq 0.25$.

**Male vs. Female Lymphoblastoid Cells**. As a simple test, we generated mRNA expression profiles from lymphoblastoid cell lines derived from 15 males and 17 females (unpublished) and sought to identify gene sets correlated with the distinctions 'male>female' and 'female>male'.

We first tested enrichment of cytogenetic gene sets ($C_1$). For the male>female comparison, we would expect to find the gene sets on chromosome Y. Indeed, GSEA produced chromosome Y and the two Y bands with at least 15 genes (Yp11 and Yq11). For the female>male comparison, we would not expect to see enrichment for bands on chromosome X because most X-linked genes are subject to dosage compensation and thus not more highly expressed in females (11).

We next considered enrichment of functional gene sets ($C_2$). The analysis yielded three biologically informative sets. One consists of genes escaping X inactivation (merged from two sources (12, 13) that largely overlap), discovering the expected

enrichment in female cells. Two additional sets consist of genes enriched in reproductive tissues (testis and uterus), which is notable inasmuch as mRNA expression was measured in lymphoblastoid cells. This result is not simply due to differential expression of genes on chromosomes X and Y, but remains significant when restricted to the autosomal genes within the sets (Supporting Information Table S3).

**p53 status in cancer cell lines**. We next examined gene expression patterns from the NCI-60 collection of cancer cell lines. We sought to use these data to identify targets of the transcription factor p53, which regulates gene expression in response to various signals of cellular stress. The mutational status of the p53 gene has been reported for 50 of the NCI60 cell lines, with 17 being classified as normal and 33 as carrying mutations in the gene (14).

We first applied GSEA to identify functional gene sets ($C_2$) correlated with p53 status. The $p53^+ > p53^-$ analysis identified five sets whose expression is correlated with normal p53 function (Table 1). All are clearly related to p53 function. The sets are (i) a biologically annotated collection of genes encoding proteins in the p53-signaling pathway that causes cell-cycle arrest in response to DNA damage; (ii) a collection of downstream targets of p53 defined by experimental induction of a temperature-sensitive allele of p53 in a lung cancer cell line; (iii) an annotated collection of genes induced by radiation, whose response is known to involve p53; (iv) an annotated collection of genes induced by hypoxia, which is known to act through a p53-mediated pathway distinct from the response pathway to DNA damage; and (v) an annotated collection of genes encoding heat-shock-protein signaling pathways that protect cells from death in response to various cellular stresses.

The complementary analysis ($p53^- > p53^+$) identifies one significant gene set: genes involved in the Ras signaling pathway. Interestingly, two additional sets that fall just short of the significance threshold contain genes involved in the Ngf and Igf1 signaling pathways. To explore whether these three sets reflect a common biological function, we examined the leading-edge subset for each gene set (defined above). The leading-edge subsets consist of 16, 11 and 13 genes respectively, with each containing four genes encoding products involved in the MAP-kinase signaling sub-pathway (MAP2K1, RAF1, ELK1, PIK3CA) (Fig. 3). This shared subset in the GSEA signal of the Ras, Ngf and Igf1

signaling pathways points to up-regulation of this component of the MAP-kinase pathway as a key distinction between the $p53^-$ and $p53^+$ tumors. (We note that a full MAP-kinase pathway appears as the ninth set on the list.)

**Acute leukemias**. We next sought to study acute lymphoid leukemia (ALL) and acute myeloid leukemia (AML), by comparing gene expression profiles that we had previously obtained from 24 ALL patients and 24 AML patients (15).

We first applied GSEA to the cytogenetic gene sets ($C_1$), with the expectation that chromosomal bands showing enrichment in one class would likely represent regions of frequent cytogenetic alteration in one of the two leukemias. The ALL>AML comparison yielded five gene sets (Table 1), which could represent frequent amplification in ALL or deletion in AML. Indeed, all five regions are readily interpreted in terms of current knowledge of leukemia.

The 5q31 band is consistent with the known cytogenetics of AML. Chromosome 5q deletions are present in most AML patients, with the critical region having been localized to 5q31 (16). The 17q23 band is a site of known genetic rearrangements in myeloid malignancies (17). The 13q14 band, containing the RB locus, is frequently deleted in AML but rarely in ALL (18). Finally, the 6q21 band contains a site of common chromosomal fragility and is commonly deleted in hematologic malignancies (19).

Interestingly, the remaining high-scoring band is 14q32. This band contains the immunoglobulin heavy chain locus, which includes over 100 genes expressed almost exclusively in the lymphoid lineage. The enrichment of 14q32 in ALL thus reflects tissue-specific expression in the lineage, rather than a chromosomal abnormality.

The reciprocal analysis (AML>ALL) yielded no significantly enriched bands. This likely reflects the relative infrequency of deletions in ALL (20). The analyses with the cytogenetic gene sets thus show that GSEA is able to identify chromosomal aberrations common in particular cancer subtypes.

**Comparing two studies of lung cancer**. A goal of GSEA is to provide a more robust way to compare independently derived gene expression data sets (possibly obtained with different platforms) and obtain more consistent results than single gene analysis. To test this, we re-analyzed data from two recent studies of lung cancer reported by our own group in Boston (21) and another group in Michigan (22). Our goal was not

to evaluate the results reported by the individual studies, but rather to examine whether common features between the data sets can be more effectively revealed by gene-set analysis rather than single-gene analysis.

Both studies determined gene-expression profiles in tumor samples from patients with lung adenocarcinomas (n = 62 for Boston; n = 86 for Michigan) and provided clinical outcomes (classified here as 'good' or 'poor' outcome). We found that no genes in either study were strongly associated with outcome at a significance level of 5% after correcting for MHT.

From the perspective of individual genes, the data from the two studies show little in common. A traditional approach is to compare the genes most highly correlated with a phenotype. We defined the gene set $S_{Boston}$ to be the top 100 genes correlated with poor outcome in the Boston study and similarly $S_{Michigan}$ from the Michigan study. The overlap is distressingly small (12 genes in common) and is barely statistically significant using a permutation test ($p = .012$). When we added a Stanford study (23) involving 24 adenocarcinomas, the three data sets share only one gene in common among the top 100 genes correlated with poor outcome (Table S4 and Fig. SF2 Supporting Information). Moreover, no clear common themes emerge from the genes in the overlaps to provide biological insight.

We then explored whether GSEA would reveal greater similarity between the Boston and Michigan lung cancer data sets. We compared the gene set from one data set, $S_{Boston}$, to the entire ranked gene list from the other. The set $S_{Boston}$ shows a strong significant enrichment in the Michigan data (NES = 1.90, $p < 0.001$). Conversely, the poor outcome set $S_{Michigan}$ is enriched in the Boston data (NES = 2.13, $p<0.001$). GSEA is thus able to detect a strong common signal in the poor outcome data (Fig. SF3 Supporting Information).

Having found that GSEA is able to detect similarities between independently derived datasets, we then went on to see if GSEA could provide biological insight, by identifying important functional sets correlated with poor outcome in lung cancer. For this purpose, we performed GSEA on the Boston and Michigan data with the $C_2$ catalog of functional gene sets. Given the relatively weak signals found by conventional single gene analysis in each study, it was not clear whether any significant gene sets would be

found by GSEA. Nonetheless, we identified a number of genes sets significantly correlated with poor outcome (FDR ≤ 0.25): 8 in the Boston data and 11 in the Michigan data (Table 1). (The Stanford data had no genes or gene sets significantly correlated with outcome; this is most likely due to the smaller number of samples and many missing values in the data.)

Moreover, there is a large overlap among the significantly enriched gene sets in the two studies. About half of the significant gene sets were shared between the two studies and an additional few, though not identical, were clearly related to the same biological process. Specifically, we find a set upregulated by telomerase (24), two different tRNA-synthesis-related sets, two different insulin-related sets, and two different p53-related sets. This makes a total of 5 out of 8 of the significant sets in Boston identical or related to 6 out of 11 in Michigan.

To provide greater insight, we next extended the analysis to include sets beyond those that met the FDR ≤ 0.25 criterion. Specifically, we considered the top-scoring 20 gene sets in each of the three studies (60 gene sets) and their corresponding leading-edge subsets in order to better understand the underlying biology in the poor outcome samples (Table S2 Supporting Information). Already in the Boston/Michigan overlap we saw evidence of telomerase and p-53 response as noted above. Telomerase activation is believed to be a key aspect of pathogenesis in lung adenocarcinoma and is well documented as prognostic of poor outcome in lung cancer.

In all three studies two additional themes emerge around rapid cellular proliferation, and amino acid biosynthesis (Table S5 Supporting Information):

(i) We see striking evidence in all three studies of the effects of rapid cell proliferation. These include sets related to Ras activation and the cell cycle as well as responses to hypoxia including angiogenesis, glycolysis, and carbohydrate metabolism. More than one third of the gene sets (23 of 60) are related to such processes. These responses have been observed in malignant tumor microenvironments where enhanced proliferation of tumor cells leads to low oxygen and glucose levels (25). The leading-edge subsets of the associated significant gene sets include hypoxia-response genes such as HIF1A, VEGF, CRK, PXN, EIF2B1, EIF2B2, EIF2S2, FADD, NFKB1, RELA, GADD45A and also Ras/MAPK activation genes (HRAS, RAF1, MAP2K1).

(ii) We find strong evidence for the simultaneous presence of increased amino acid biosynthesis, *mTor* signaling, and up-regulation of a set of genes down-regulated by both amino acid deprivation and rapamycin treatment (26). Supporting this are 17 gene sets associated with amino acid and nucleotide metabolism, immune modulation and *mTor* signaling. Based on these results, one might speculate that rapamycin treatment might have an effect on this specific component of the poor outcome signal. We note there is evidence of the efficacy of rapamycin in inhibiting growth and metastatic progression of Non-Small Cell Lung Cancer in mice and human cell lines (27).

Our analysis shows that we find much greater consistency across the three lung datasets and by using GSEA than single gene analysis. Moreover, we are better able to generate compelling hypotheses for further exploration. In particular, 40 of the 60 top scoring gene sets across these three studies give a consistent picture of underlying biological processes in poor outcome cases.

**6. GSEA-P software and MSigDB gene sets**

To facilitate the use of GSEA, we have developed resources that are freely available at (www.broad.mit.edu/GSEA). The site contains the GSEA-P software; the Molecular Signatures Database (MSigDB 1.0); and accompanying documentation.

The software is available as (i) a platform-independent desktop application with a graphical user interface; (ii) programs in R and in Java that advanced users may incorporate into their own analyses or software environments; (iii) an analytic module in our GenePattern microarray analysis package (www.broad.mit.edu/genepattern) (iv) a future web-based GSEA server to allow users to run their own analysis directly on the website. A detailed example of the output format of GSEA is available on the site, as well as in Supporting Information.

**7. Use of GSEA in other settings**

We have focused above on the use of GSEA to analyze a ranked gene list reflecting differential expression between two classes, each represented by a large number of samples. However, the method can be applied to ranked gene lists arising in other settings.

Genes may be ranked based on the differences seen in a small data set, with too few samples to allow rigorous evaluation of significance levels by permuting the class labels. In these cases, a *P*-value can be estimated by permuting the genes, with the result that genes are randomly assigned to the sets while maintaining their size. This approach is not strictly accurate: because it ignores gene-gene correlations, it will overestimate the significance levels and may lead to false positives. Nonetheless, it can be useful for hypothesis generation. The GSEA-P software supports this option.

Genes may also be ranked based on how well their expression correlates with a given target pattern (such as the expression pattern of a particular gene). In Lamb et al. (28), a GSEA-like procedure was used to demonstrate the enrichment of a set of targets of cyclin D1 list ranked by correlation with the profile of cyclin D1 in a compendium of tumor types. Again, approximate P-values can be estimated by permutation of genes.

**8. Discussion**

Traditional strategies for gene expression analysis have focused on identifying individual genes that exhibit differences between two states of interest. While useful, they fail to detect biological processes - such as metabolic pathways, transcriptional programs, and stress responses – that are distributed across an entire network of genes and subtle at the level of individual genes.

We previously introduced GSEA to analyze such data at the level of gene sets. The method was initially used to discover metabolic pathways altered in human diabetes and was subsequently applied to discover processes involved in diffuse large B cell lymphoma (29), nutrient-sensing pathways involved in prostate cancer (30), and in comparing the expression profiles of mouse to those of humans (31). In the current paper, we have refined the original approach into a sensitive, robust analytical method and tool with much broader applicability along with a large database of gene sets. GSEA can clearly be applied to other large-scale datasets such as serum proteomics data, genotyping information, or metabolite profiles.

GSEA features a number of advantages when compared to single gene methods. First, it eases the interpretation of a large-scale experiment by identifying pathways and processes. Rather than focus on high scoring genes (which can be poorly annotated and

may not be reproducible), researchers can focus on gene sets. These tend to be more reproducible and more interpretable. Second, when the members of a gene set exhibit strong cross-correlation, GSEA can boost the signal to noise ratio and make it possible to detect modest changes in individual genes. Third, the leading-edge analysis can help define gene subsets to elucidate the results.

Several other tools have recently been developed to analyze gene expression using pathway or ontology information, e.g., (32), (33), (34). Most determine whether a group of differentially expressed genes is enriched for a pathway or ontology term by using overlap statistics such as the cumulative hypergeometric distribution. We note that this approach is not able to detect the OXPHOS results discussed above ($P = .08$, $FDR = .50$). GSEA differs in two important regards. First, GSEA considers all the genes in an experiment, not only those above an arbitrary cutoff in terms of fold-change or significance. Second, GSEA assesses the significance by permuting the class labels; this preserves gene-gene correlations and thus provides a more accurate null model.

The real power of GSEA, however, lies in its flexibility. We have created an initial molecular signature database consisting of over 1000 gene sets. These include sets based on biological pathways, chromosomal location, upstream *cis*-motifs, responses to a drug treatment, or expression profiles in previously generated microarray datasets. Further sets can be created through genetic and chemical perturbation, computational analysis of genomic information, and additional biological annotation. In addition, GSEA itself could be used to refine manually curated pathways and sets by identifying the leading-edge sets that are shared across diverse experimental datasets. As such sets are added, tools such as GSEA will help link prior knowledge to newly generated data and thereby help uncover the collective behavior of genes in states of health and disease.

## 8. Appendix: Mathematical Description of Methods

**Inputs to GSEA:**

1. Expression dataset $D$ with $N$ genes and $k$ samples.

2. Ranking procedure to produce Gene List $L$. Includes a correlation (or other ranking metric,) and a phenotype or profile of interest $C$. We use only one probe per gene to prevent over-estimation of the enrichment statistic (Supporting Information and Table

S6).

3. An exponent *p* to control the weight of the step.

4. Independently derived Gene Set *S* of $N_H$ genes (e.g., a pathway, a cytogenetic band, a GO category). In the analyses above, we used only genes sets with at least 15 members to focus on robust signals (78% of MSigDB) (Table S1).

**Enrichment Score *ES(G)*:**

1. Rank order the *N* genes in *D* to form $L = \{g_1, \ldots, g_N\}$ according to the correlation, $r(g_j) = r_j$, of their expression profiles with *C* using *M*.

2. Evaluate the fraction of genes in *S* ("hits") weighted by their correlation and the fraction of genes not in *S* ("misses") present up to a given position *i* in *L*.

$$P_{hit}(S,i) = \sum_{\substack{g_j \in S \\ j \le i}} \frac{|r_j|^p}{N_R} \qquad \text{where} \quad N_R = \sum_{g_j \in S} |r_j|^p$$

$$P_{miss}(S,i) = \sum_{\substack{g_j \notin S \\ j \le i}} \frac{1}{(N - N_H)}$$

The *Enrichment Score (ES)* is the maximum deviation from zero of $P_{hit}$ - $P_{miss}$. For a randomly distributed *S, ES(S)* will be relatively small but if it is concentrated at the top or bottom of the list, or otherwise non-randomly distributed, then *ES(S)* will be correspondingly high. When *p=0*, this reduces to the standard Kolmogorov-Smirnov statistic; when *p=1*, we are weighting the genes in *S* by their correlation with *C* normalized by the sum of the correlations over all the genes in *S*. We set *p=1* for the examples in this paper.

**Estimating Significance:**

We assess the significance of an observed *ES* by comparing it with the set of scores $ES_{NULL}$ computed with randomly assigned phenotypes.

1. Randomly assign the original phenotype labels to samples, reorder genes, re-compute *ES(S)*.

2. Repeat step 1 for 1000 permutations, and create a histogram of the corresponding enrichment scores $ES_{NULL}$.

3. Estimate nominal *P*-value for *S* from $ES_{NULL}$ using the positive or negative portion of the distribution corresponding to the sign of the observed *ES(S)*.

**Multiple Hypothesis Testing:**

1. Determine *ES(S)* for each gene set in the collection or database.

2. For each *S* and 1000 fixed permutations π of the phenotype labels re-order the genes in *L* and determine *ES(S, π)*.

3. Adjust for variation in gene set size:

Normalize the *ES(S, π)* and the observed *ES(S)*, separately rescaling the positive and negative scores by dividing by the mean of the *ES(S, π)*. This yields the normalized scores *NES(S, π)* and *NES(S)*. (See Supporting Information.)

4. Compute False Discovery Rate (FDR). Control the ratio of false positives to the total number of gene sets attaining a fixed level of significance. This is done separately for positive and negative *NES(S)* and *NES(S, π))*.

Create a histogram of all *NES(S, π)* over all *S* and π. Use this null distribution to compute an FDR q-value, for a given $NES(S) = NES^* \geq 0$ .

$$\frac{\%\text{ of all } (S,\pi) \text{ with } NES(S,\pi) \geq 0 \text{ whose } NES(S,\pi)) \geq NES^*}{\%\text{ of observed } S \text{ with } NES(S) \geq 0 \text{ whose } NES(S) \geq NES^*} \quad ,$$

and similarly if $NES(S) = NES^* \leq 0$.

**9. Acknowledgements**

We gratefully acknowledge discussions with or data from D. Altshuler, N. Patterson, J. Lamb, X. Xie, J-Ph. Brunet, S. Ramaswamy, J-P. Bourquin, B. Sellers, L. Sturla, and C. Nutt; and helpful comments from reviewers.

**Main Paper Captions**

**Figure 1. GSEA Overview.** This figure illustrates the original GSEA method from (4). A) An expression dataset sorted by correlation with phenotype, the corresponding heat map, and the "gene tags", i.e., location of genes from a set *S* within the sorted list. B) Plot of the running sum for *S* in the dataset including the location of the maximum enrichment score (ES) and the leading-edge subset.

**Figure 2. Enrichment Score Behavior.** The behavior of the GSEA score using the original method (4) according to a gene set's distribution on the ranked list. A) The distribution of 3 gene sets, from the C2 functional collection, in the list of genes in the Male/Female Lymphoblastoid cell line example ranked by their correlation with gender: S1, a set of Chromosome X inactivation genes; S2, a pathway describing vitamin c import into neurons; S3, related to chemokine receptors expressed by T helper cells. The figure shows plots of the running sum for the 3 gene sets: S1 is significantly enriched in females as expected; S2 is randomly distributed and scores poorly; S3 is not enriched at the top of the list but is non-random so scores well. Arrows show the location of the maximum enrichment score and the point where the correlation (signal to noise ratio) crosses zero. B) Comparison of the nominal p-values for S1, S2, S3 using the original and new method. The new method reduces the significance of sets like S3.

**Figure 3. Leading edge overlap for p53- study.** This plot shows the *ras, ngf, igf1* gene sets correlated with $P53^{-}$ clustered by their leading-edge subsets indicated in dark blue. A common subgroup of genes, apparent as a dark vertical stripe, consists of MAP2K1, PIK3CA, ELK1 and RAF1 and represents a subsection of the MAPK pathway.

**Table 1**. **Summary of GSEA results with FDR ≤ 0.25.** For detailed results see Table S2 in Supporting Information.

**Bibliography**


1. Schena, M., Shalon, D., Davis, R. W. & Brown, P. O. (1995) *Science* **270,** 467-70.
2. Lockhart, D. J., Dong, H., Byrne, M. C., Follettie, M. T., Gallo, M. V., Chee, M. S., Mittmann, M., Wang, C., Kobayashi, M., Horton, H., et al. (1996) *Nat Biotechnol* **14,** 1675-80.
3. Fortunel, N. O., Otu, H. H., Ng, H. H., Chen, J., Mu, X., Chevassut, T., Li, X., Joseph, M., Bailey, C., Hatzfeld, J. A., et al. (2003) *Science* **302,** 393; author reply 393.
4. Mootha, V. K., Lindgren, C. M., Eriksson, K. F., Subramanian, A., Sihag, S., Lehar, J., Puigserver, P., Carlsson, E., Ridderstrale, M., Laurila, E., et al. (2003) *Nat Genet* **34,** 267-73.
5. Patti, M. E., Butte, A. J., Crunkhorn, S., Cusi, K., Berria, R., Kashyap, S., Miyazaki, Y., Kohane, I., Costello, M., Saccone, R., et al. (2003) *Proc Natl Acad Sci U S A* **100,** 8466-71.
6. Petersen, K. F., Dufour, S., Befroy, D., Garcia, R. & Shulman, G. I. (2004) *N Engl J Med* **350,** 664-71.
7. Hollander, M. & Wolfe, D. A. (1999) *Nonparametric statistical methods* (J. Wiley, New York).
8. Benjamini, Y., Drai, D., Elmer, G., Kafkafi, N. & Golani, I. (2001) *Behav Brain Res* **125,** 279-84.
9. Reiner, A., Yekutieli, D. & Benjamini, Y. (2003) *Bioinformatics* **19,** 368-75.
10. Xie, X., Lu, J., Kulbokas, E. J., Golub, T. R., Mootha, V., Lindblad-Toh, K., Lander, E. S. & Kellis, M. (2005) *Nature* **434,** 338-45.
11. Plath, K., Mlynarczyk-Evans, S., Nusinow, D. A. & Panning, B. (2002) *Annu Rev Genet* **36,** 233-78.
12. Carrel, L., Cottle, A. A., Goglin, K. C. & Willard, H. F. (1999) *Proc Natl Acad Sci U S A* **96,** 14440-4.
13. Disteche, C. M., Filippova, G. N. & Tsuchiya, K. D. (2002) *Cytogenet Genome Res* **99,** 36-43.
14. Olivier, M., Eeles, R., Hollstein, M., Khan, M. A., Harris, C. C. & Hainaut, P. (2002) *Hum Mutat* **19,** 607-14.
15. Armstrong, S. A., Staunton, J. E., Silverman, L. B., Pieters, R., den Boer, M. L., Minden, M. D., Sallan, S. E., Lander, E. S., Golub, T. R. & Korsmeyer, S. J. (2002) *Nat Genet* **30,** 41-7.
16. Zhao, N., Stoffel, A., Wang, P. W., Eisenbart, J. D., Espinosa, R., 3rd, Larson, R. A. & Le Beau, M. M. (1997) *Proc Natl Acad Sci U S A* **94,** 6948-53.
17. Barbouti, A., Hoglund, M., Johansson, B., Lassen, C., Nilsson, P. G., Hagemeijer, A., Mitelman, F. & Fioretos, T. (2003) *Cancer Res* **63,** 1202-6.
18. Tanaka, K., Arif, M., Eguchi, M., Guo, S. X., Hayashi, Y., Asaoku, H., Kyo, T., Dohy, H. & Kamada, N. (1999) *Leukemia* **13,** 1367-73.
19. Morelli, C., Karayianni, E., Magnanini, C., Mungall, A. J., Thorland, E., Negrini, M., Smith, D. I. & Barbanti-Brodano, G. (2002) *Oncogene* **21,** 7266-76.
20. Mrozek, K., Heerema, N. A. & Bloomfield, C. D. (2004) *Blood Rev* **18,** 115-36.

21. Bhattacharjee, A., Richards, W. G., Staunton, J., Li, C., Monti, S., Vasa, P., Ladd, C., Beheshti, J., Bueno, R., Gillette, M., et al. (2001) *Proc Natl Acad Sci U S A* **98,** 13790-5.
22. Beer, D. G., Kardia, S. L., Huang, C. C., Giordano, T. J., Levin, A. M., Misek, D. E., Lin, L., Chen, G., Gharib, T. G., Thomas, D. G., et al. (2002) *Nat Med* **8,** 816-24.
23. Garber, M. E., Troyanskaya, O. G., Schluens, K., Petersen, S., Thaesler, Z., Pacyna-Gengelbach, M., van de Rijn, M., Rosen, G. D., Perou, C. M., Whyte, R. I., et al. (2001) *Proc Natl Acad Sci U S A* **98,** 13784-9.
24. Smith, L. L., Coller, H. A. & Roberts, J. M. (2003) *Nat Cell Biol* **5,** 474-9.
25. Acker, T. & Plate, K. H. (2002) *J Mol Med* **80,** 562-75.
26. Peng, T., Golub, T. R. & Sabatini, D. M. (2002) *Mol Cell Biol* **22,** 5575-84.
27. Boffa, D. J., Luan, F., Thomas, D., Yang, H., Sharma, V. K., Lagman, M. & Suthanthiran, M. (2004) *Clin Cancer Res* **10,** 293-300.
28. Lamb, J., Ramaswamy, S., Ford, H. L., Contreras, B., Martinez, R. V., Kittrell, F. S., Zahnow, C. A., Patterson, N., Golub, T. R. & Ewen, M. E. (2003) *Cell* **114,** 323-34.
29. Monti, S., Savage, K. J., Kutok, J. L., Feuerhake, F., Kurtin, P., Mihm, M., Wu, B., Pasqualucci, L., Neuberg, D., Aguiar, R. C., et al. (2004) *Blood*.
30. Majumder, P. K., Febbo, P. G., Bikoff, R., Berger, R., Xue, Q., McMahon, L. M., Manola, J., Brugarolas, J., McDonnell, T. J., Golub, T. R., et al. (2004) *Nat Med* **10,** 594-601.
31. Sweet-Cordero, A., Mukherjee, S., Subramanian, A., You, H., Roix, J. J., Ladd-Acosta, C., Mesirov, J., Golub, T. R. & Jacks, T. (2005) *Nat Genet* **37,** 48-55.
32. Doniger, S. W., Salomonis, N., Dahlquist, K. D., Vranizan, K., Lawlor, S. C. & Conklin, B. R. (2003) *Genome Biol* **4,** R7.
33. Zhong, S., Storch, K. F., Lipan, O., Kao, M. C., Weitz, C. J. & Wong, W. H. (2004) *Appl Bioinformatics* **3,** 261-4.
34. Berriz, G. F., King, O. D., Bryant, B., Sander, C. & Roth, F. P. (2003) *Bioinformatics* **19,** 2502-4.

Figure 1

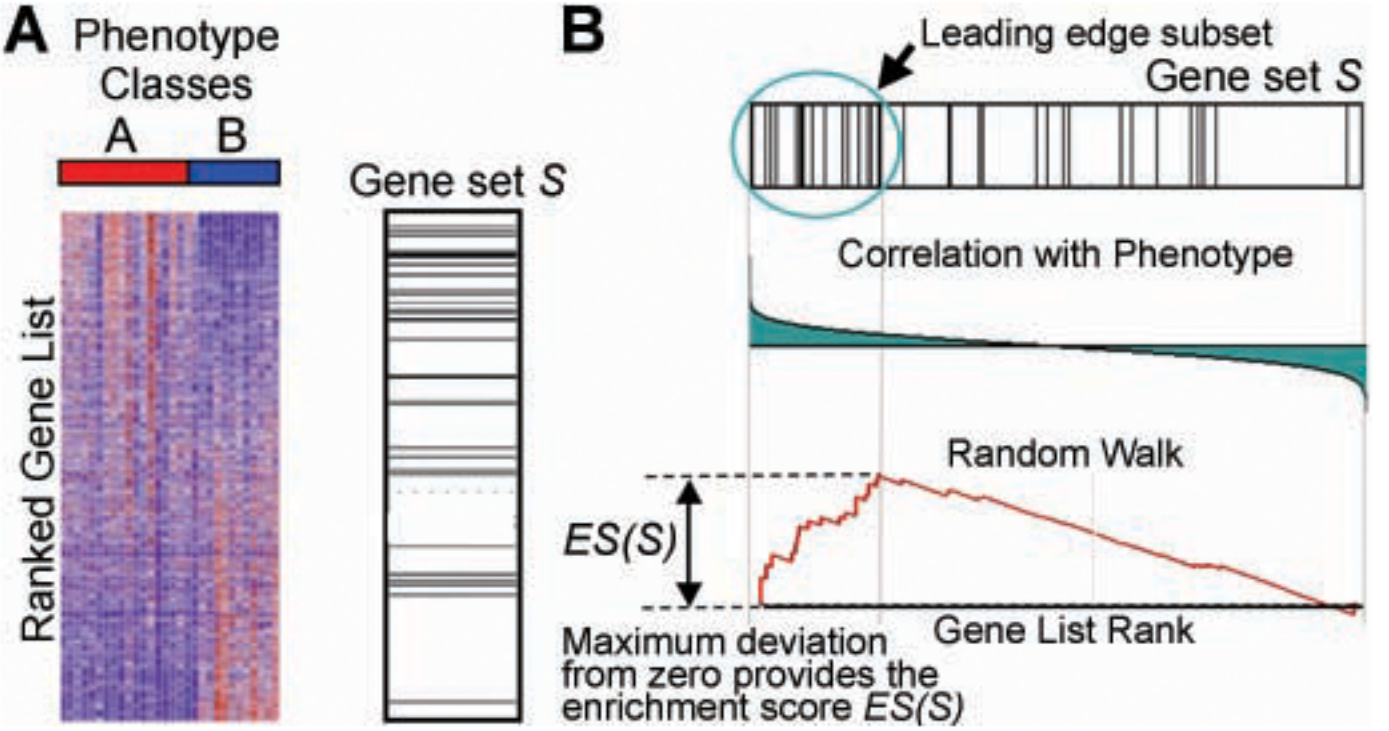


Figure 2

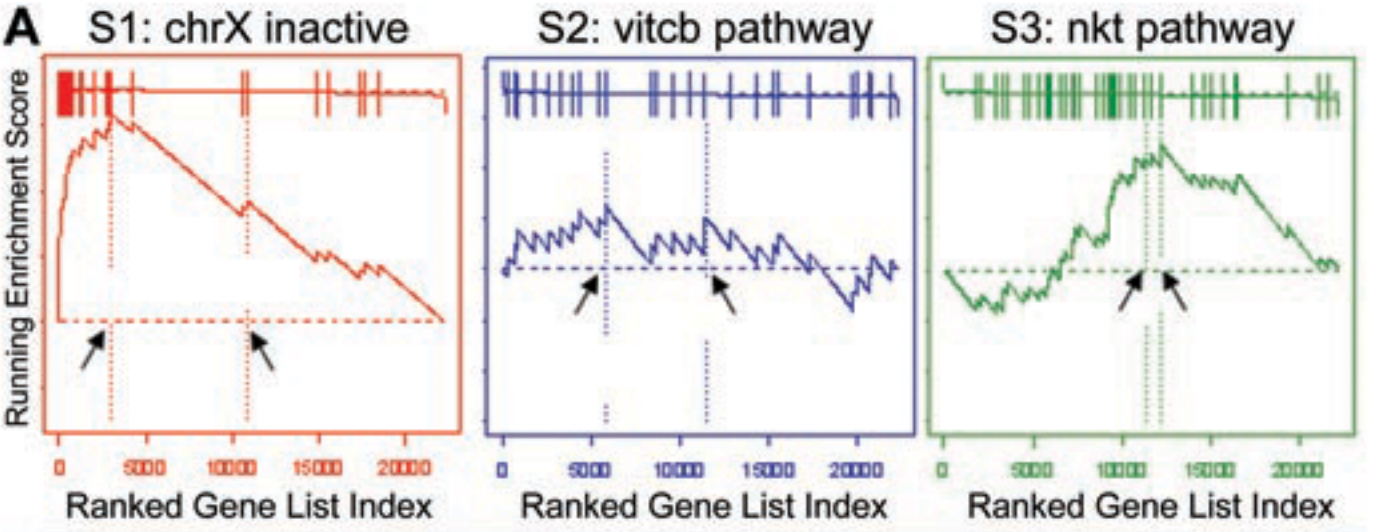


B

| Gene Set | Original Method Nominal p-value | New Method Nominal p-value |
|---|---|---|
| S1: chrX inactive | 0.007 | <0.001 |
| S2: vitcb pathway | 0.51 | 0.38 |
| S3: nkt pathway | 0.023 | 0.54 |

Figure 3

Table 1

| GENE SET | FDR |
|---|---|
| **Dataset: Lymphoblast Cell Lines** | |
| **Enriched in Males** | |
| chrY | <0.001 |
| chrYp11 | <0.001 |
| chrYq11 | <0.001 |
| Testis expressed genes | 0.012 |
| **Enriched in Females** | |
| X inactivation genes | <0.001 |
| Female reproductive tissue expressed genes | 0.045 |
| **Dataset: p53 status in NCI-60 Cell Lines** | |
| **Enriched in p53 Mutant** | |
| Ras signaling pathway | 0.171 |
| **Enriched in p53 Wild Type** | |
| Hypoxia and p53 in the Cardiovascular system | <0.001 |
| Stress induction of HSP regulation | <0.001 |
| p53 signaling pathway | <0.001 |
| p53 upregulated genes | 0.013 |
| Radiation sensitivity genes | 0.078 |
| **Dataset: Acute Leukemias** | |
| **Enriched in ALL** | |
| chr6q21 | 0.011 |
| chr5q31 | 0.046 |
| chr13q14 | 0.057 |
| chr14q32 | 0.082 |
| chr17q23 | 0.071 |
| **Dataset: Lung Cancer Outcome, Boston Study** | |
| **Enriched in Poor Outcome** | |
| Hypoxia and p53 in the Cardiovascular system | 0.050 |
| Aminoacyl tRNA biosynthesis | 0.144 |
| Insulin upregulated genes | 0.118 |
| tRNA synthetases | 0.157 |
| Leucine deprivation downregulated genes | 0.144 |
| Telomerase upregulated genes | 0.128 |
| Glutamine deprivation downregulated genes | 0.146 |
| Cell cycle checkpoint | 0.216 |
| **Dataset: Lung Cancer Outcome, Michigan Study** | |
| **Enriched in Poor Outcome** | |
| Glycolysis Gluconeogenesis | 0.006 |
| vegf pathway | 0.028 |
| Insulin upregulated genes | 0.147 |
| Insulin signalling | 0.170 |
| Telomerase upregulated genes | 0.188 |
| Glutamate metabolism | 0.200 |
| Ceramide pathway | 0.204 |
| p53 signalling | 0.179 |
| tRNA synthetases | 0.225 |
| Breast cancer estrogen signalling | 0.250 |
| Aminoacyl tRNA biosynthesis | 0.229 |

**Supporting Information for:**

# Gene Set Expression Analysis: A knowledge-based approach for interpreting mRNA profiles

**Aravind Subramanian, Pablo Tamayo, Vamsi Mootha, Sayan Mukherjee, Benjamin L. Ebert, Michael A. Gillette, Amanda Paulovich, Scott L. Pomeroy, Todd R. Golub, Eric S. Lander, and Jill P. Mesirov**

Contents of Supporting Information:

1 Supporting Tables and Figures (attached) ..... 2
2 Datasets: description, preprocessing and normalization. ..... 3
2.1 Gene probe to gene symbol reduction ..... 3
2.2 Description of data sets ..... 3
2.2.1 Gender Dataset. ..... 3
2.2.2 P53 NCI-60 Dataset. ..... 4
2.2.3 Leukemia ALL/AML Dataset. ..... 4
2.2.4 Lung Cancer Datasets ..... 4
3 Additional detail on gene set collections. ..... 4
4 Additional detail on the GSEA method ..... 5
5 Description of GSEA output. ..... 8
6 Post GSEA analysis: leading-edge subset similarity, clustering, and assignment ..... 10
7 Original GSEA method from Mootha et al. 2003. ..... 11
8 GSEA-P R program ..... 11

## 1 Supporting Tables and Figures (attached)

### Table Captions

**Table S1**. **MSigDB Collections.** This table gives the number of gene sets in each collection, the numbers of sets that pass the size thresholds (min=15, max=500), and the final number of sets used in the examples in the main paper.

**Table S2. Summary of GSEA results.** The top 20 scoring gene sets for all of the examples described in the paper. Entries in boldface correspond to sets with FDR ≤ 0.25.

**Table S3. Functional autosomal gene set enrichment with respect to gender.** This table shows the GSEA results for the gender dataset using the functional collection C2 after restricting the gene set membership to autosomal genes.

**Table S4**. **Single gene overlaps in lung studies.** This table shows the pairwise overlap between the top 100 genes correlated with poor outcome in the Michigan, Boston, and Stanford datasets as depicted in Figure SF2. Pair wise overlap is determined using genes which appear on both studies' technology platforms. Restricting to genes on all 3 platforms would reduce the gene space by 50% in the Michigan study, and by 70% in the Boston and Stanford studies.

**Table S5**. **Functional overlaps of top 20 gene sets enriched in poor outcome in the 3 lung cancer data sets.** This table organizes the gene sets enriched in poor outcome in lung shown in Table S2 according to their pathway, process/context, and major biological response/theme.

**Table S6**. **Probe set to gene ID reduction.** This table shows the distribution of probe sets per gene id in the 3 Affymetrix chip types used on the datasets in the paper. The data displayed is binned by the number of probes per gene. The majority of the over-representation arises from 2 or 3 probes per gene. In our analyses we chose the maximally expressed probe as the single representative of the corresponding gene.

### Figure Captions

**Figure SF1. Asymmetry of GSEA results due to unbalanced global phenotype expression and gene set collection bias.** A) Shows the GSEA observed and null distributions when a collection of random gene sets with the same number and size distribution as the functional C2 collection is run against the diabetes dataset from Mootha et al. 2003. Random sets have small biases (left) so that only a modest correction is made by the normalization procedure (right). The middle of the observed and null distributions coincide as they should. B) Here the actual C2 collection is run against the diabetes data set and we clearly see the bias in the observed distribution caused by unequal representation gene sets in the two phenotypes. Normalizing the positive and negative side of the distribution independently helps to ameliorate this bias. C) The

Leukemia dataset (1) illustrates bias in the gene expression correlation profiles between the two phenotypes. On the ALL side there are more markers and they are more highly correlated markers (left). Again independent normalization of positive and negative scoring sets decreases this bias (right).

**Figure SF2.** Single gene overlaps in lung cancer studies. This Venn diagram shows the pairwise and 3-way overlap between the top 100 genes correlated with poor outcome in the Michigan, Boston, and Stanford datasets. Pairwise overlap is determined using genes which appear on both studies' technology platforms. 3-way overlap is the overlap of the pairwise overlaps. Restricting to genes on all 3 platforms would reduce the gene space by 50% in the Michigan study, and by 70% in the Boston and Stanford studies.

**Figure SF3.** Enrichment plots for poor outcome signatures across lung cancer studies. Enrichment plots for the $S_{Boston}$ and $S_{Michigan}$ signatures of poor outcome against the Michigan and Boston data sets respectively. Signatures are defined as those genes in the set of top 100 outcome markers that are also represented in the other study. The signatures are scored against data from genes represented in both studies.

**Figure SF4**. Enrichment plots for the original and current GSEA methods for the set of genes upregulated by p53 in the p53 wild type phenotype.

## 2 Datasets: description, preprocessing and normalization.

### 2.1 Gene probe to gene symbol reduction

In all data sets, for each sample the expression values of all probe set ids for a given gene were reduced to a single value by taking the maximum expression value. By this process, the 22,283 features on the U133A chip (diabetes and gender examples) were reduced by 30% to 15,060 features, the 12,625 features on the HGU95Av2 chip (p53, leukemia, & lung Boston) were reduced by 18% to 10,104 features and the 7,129 features on HU6800 (lung Michigan) were reduced by 10% to 6,314 features (see Table S6). Probe set ids which have no known mapping to a gene symbol were left unchanged in the dataset (on average 10% of the probe sets on a chip). This probe reduction method is included in the GSEA-P Java package.

### 2.2 Description of data sets.

#### 2.2.1 Gender Dataset.

This dataset is unpublished (Paulovich et al.) The U133A CEL files were scaled using Broad Institute's ResFileManager software. Different array intensities were normalized by choosing a linear fit to the median scan (all genes). No further preprocessing was done except for gene probe reduction as described in section 2.1 above.

### 2.2.2 P53 NCI-60 Dataset.

The NCI 60 dataset was downloaded from the DTP website (http://dtp.nci.nih.gov/mtargets/download.html). No preprocessing was done except for gene probe reduction as described in section 2.1 above.

### 2.2.3 Leukemia ALL/AML Dataset.

The Leukemia dataset was downloaded from (1) (http://www.broad.mit.edu/cgi-bin/cancer/publications/pub_paper.cgi?mode=view&paper_id=63). No preprocessing was done except for gene probe reduction as described in section 2.1 above.

### 2.2.4 Lung Cancer Datasets

**Michigan:** The Beer et al. (2) dataset was downloaded from http://dot.ped.med.umich.edu:2000/ourimage/pub/Lung/index.html No further preprocessing was done except for gene probe reduction as described in section 2.1 above.

**Boston:** The Bhattacharjee et al. (3) dataset was downloaded from http://www.broad.mit.edu/cgi-bin/cancer/publications/pub_paper.cgi?mode=view&paper_id=62. We extracted those lung adenocarcinomas samples for which outcome information was provided. No further preprocessing was done except for gene probe reduction as described in section 2.1 above.

**Stanford:** The Stanford dataset from Garber et al. (4) was downloaded from http://genome-www.stanford.edu/lung_cancer/adeno/data.shtml. Missing values were replaced by zeroes. No further preprocessing was done except for gene probe reduction as described in section 2.1 above.

## 3 Additional detail on gene set collections.

- **Functional sets (C2, 522 gene sets)**. The sources for sets in the C2 collection are:

1 BioCarta: http://www.biocarta.com/
2 Signaling pathway database: http://www.grt.kyushu-u.ac.jp/spad/menu.html
3 Signaling gateway: http://www.signaling-gateway.org
4 Signal transduction knowledge environment: http://stke.sciencemag.org/
5 Human protein reference database: http://www.hprd.org/
6 GenMAPP: http://www.genmapp.org/

7 Gene ontology: http://www.geneontology.org/
8 Sigmal Aldrich pathways: http://www.sigmaaldrich.com/Area_of_Interest/Biochemicals/Enzyme_Explorer/Key_Resources.html
9 Gene arrays, BioScience corporation: http://www.superarray.com
10 Human cancer genome anatomy consortium: http://cgap.nci.nih.gov/

- **Regulatory-motif sets (C3, 57 gene sets).** This catalog is based on our recent work reporting 57 commonly conserved regulatory motifs in the promoter regions of human genes (5). Some of the sites correspond to known transcription-related factors (such as SP1 and p53), while others are newly described. For each 8-mer motif, we identified the set of human genes that contain at least one occurrence of the motif that is conserved in the orthologous location in the human, mouse, rat and dog genomes. These gene sets make it possible to link changes in a microarray experiment to a conserved, putative cis-regulatory element.

- **Neighborhood sets (C4, 427 gene sets).** We curated a list of 380 cancer associated genes internally and from a published cancer gene database (6). We then defined neighborhoods around these genes in four large gene expression datasets:

    1) Novartis normal tissue compendium (7)
    2) Novartis carcinoma compendium (8)
    3) Global cancer map (9)
    4) An internal large compendium of gene expression datasets including many of our in-house Affymetrix U95 cancer samples (1693 in all) from a variety of cancer projects representing many different tissue types, mainly primary tumors, such as prostate, breast, lung, lymphoma, leukemia, etc.

  Using the profile of a given gene as a template, we ordered every other gene in the dataset by its Pearson correlation coefficient. We applied a cutoff of $R \geq 0.85$ to extract correlated genes. The calculation of neighborhoods is done independently in each compendium. In this way a given oncogene may have up to four "types" of neighborhoods according to the correlation present in each compendium. Neighborhoods with less than 25 genes at this threshold were omitted yielding the final 427 sets.

## 4 Additional details on the GSEA method

Here we elaborate on some aspects of the GSEA method that are more technical and were not described in great amount of detail in the main text due to space constraints.

### 4.1 Calculation of an enrichment score.

**4.1.1 Setting of the enrichment weighting exponent p**. In the examples described in the

text, and in many other examples not reported, we found that p=1 (weighting by the correlation) is a very reasonable choice that allows significant gene sets with less than perfect coherence, i.e., only a subset of genes in the set are coordinately expressed, to score well. In other less common specific circumstances one may want to use a different setting and for this reason the GSEA-P program accepts *p* as an input parameter. For example, if one is interested in penalizing sets for lack of coherence or to discover sets with any type of non-random distribution of tags, a value p<1 might be appropriate. On the other hand if one uses sets with large number of genes and only a small subset of those is expected to be coherent then one could consider using p>1. Our recommendation is to use p=1 and use other settings only if you are very experienced with the method and its behavior.

**4.1.2 Benefits of weighting by gene correlation.**

Most gene sets show some amount of coherent behavior but are far from being perfectly coherent. For example in Figure SF4 we show the enrichment plot for the set of genes up-regulated by p53 in the p53 wild type phenotype. This set is one of those that is significantly enriched using the current GSEA method. However if we use the original constant weight GSEA analysis this set is not significant. This is a problem because we would expect such a set to be enriched for the p53 wild type phenotype. From the figure we can see that the 40 genes in the set are not uniformly coherent, but rather split into two co-expressed groups with some additional scatter. The use of equal weighting tends to over-penalize this lack of coherence and does not produce a significant ES for this gene set, even though a significant subset of its genes are near the top of the list.

**4.2 Multiple Hypothesis Testing.**

**4.2.1 Adjusting for variation in gene set size.** As described in the Appendix of the main text, when adjusting for variation in gene set size we normalize the *ES(S, π)* for a given *S*, separately rescaling the positive and negative scores by dividing by their mean value. This yields the normalized scores *NES(S, π)* and *NES(S)*.
This gene set size normalization procedure appropriately aligns the null distributions for different gene sets and is motivated by the asymptotic multiplicative scaling of the Kolmogorov-Smirnov distribution as a function of size (10). Here we will make a brief digression to elaborate on this subject.

The analytic form of the Kolmogorov-Smirnov distribution scaling with gene set size can be derived from the expectation value of the approximated distribution function of the enrichment statistic:

$$\Pr\left(\mathrm{ES}\left(N, N_H\right) < \lambda\right) = \sum_{k=-\infty}^{\infty} \left(-1\right)^k \exp\left(-2k^2\lambda^2 n\right), \quad n = \frac{(N - N_H)N_H}{N},$$

where $\lambda$ is the enrichment score, $N$ is the number of genes in the gene list and $N_H$ the number of genes in the gene set. The number of terms required for the above series to converge depends on $\lambda$. As $\lambda$ approaches zero, more terms are required. From the

above equation, we can compute the following density function for the enrichment statistic

$$\rho(\lambda) = 4\sum_{k=-\infty}^{\infty} (-1)^{k+1} k^2 n\lambda \exp\left(-2k^2\lambda^2 n\right).$$

Notice the multiplicative scaling of the distribution with n, and for large gene lists ($N >> N_H$ ) with $N_H$.
The average enrichment score is simply the expectation (integral from $\lambda = 0$ to 1), with respect to the above density:

$$\overline{ES} = \mathrm{E}_{\rho(\lambda)}\, ES\left(N, N_H\right) = \int_{\lambda=0}^{1} \lambda\rho(\lambda)\, d\lambda$$
$$= 4\sum_{k=-\infty, k\neq 0}^{\infty} (-1)^{k+1} \left( \tfrac{1}{4}\exp\left(-2k^2 n\right) - \frac{\sqrt{2\pi}}{16}\frac{\mathrm{erf}\left(\sqrt{2n}k\right)}{k\sqrt{n}} \right).$$

Where erf is the "error function" (integral of the normal distribution).

The mean values of the null distribution of enrichment scores computed with this approximation are quite consistent with our actual empirical results when using GSEA unweighted enrichment scores (p=0). Therefore if we were only performing unweighted GSEA and permuting the genes we could analytically compute the normalization factor using the equation above. However our standard practice is to use weighting and to permute the phenotype labels, therefore this expression is not entirely accurate.

For example when using GSEA weighted scores (p=1) the empirical mean values are about 5 times smaller. This expected reduction in “effective” gene set size is the direct effect of gene-gene correlations. Notice that these correlations are preserved by the phenotype label permutation and are also relevant when using the correlation profiles as part of the weighted GSEA enrichment score calculation. Despite the change in the mean, the shape of the distribution is still very much the same and multiplicative scaling works well empirically for the gene set size normalization.

**4.2.2 Computing significance using positive or negative sides of the observed and null bimodal ES distributions:** As mentioned in the main text the use of a weighted enrichments score helps make the current GSEA method more sensitive and eliminates some of the limitations of the original GSEA method; however, it also makes more apparent any lack of symmetry in the distribution of observed ES values. This intrinsic asymmetry can be due to class specific biases either in the *gene correlations* or in the population of the *gene set collection* itself (Fig. SF1). Specifically, many more genes may be highly correlated with one phenotype, or the collection of gene sets may contain more that are related to one of the two phenotypes. On the other hand, constructing the null using random phenotype assignments tends to produce a more symmetric distribution that may not exactly coincide with the bulk, non-extreme part of the distribution of the

observed values. To address this, we determine significance and adjust for multiple hypotheses testing by independently using the positive and negative sides of the observed and null bimodal ES distributions. In this way the significance tests (nominal p-value, FWER and FDR) are single tail tests on the appropriate (positive/negative) side of the null distribution.

**4.2.3 Family Wise Error Rate (FWER).** The use of the family-wise-error rate (FWER), which controls the probability of a false positive, to correct for MHT in the original GSEA method is overly conservative and often yields no statistically significant gene sets. For example the analysis results using the original GSEA method do not produce any significant set (FWER < 0.05) on either side in the Gender, Leukemia and p53 examples. Nonetheless the GSEA-P program also computes the family wise error by creating a histogram of the maximum *NES(S, π)* over all *S* for each π using the positive or negative values corresponding to the sign of the observed *NES(S)*. This null distribution is then used to compute an FWER p-value.

## 5 Description of GSEA output.

The output of the GSEA-P software includes a list of the gene sets sorted by their *NES* values along with their nominal and FWER p-values and their FDR q-values.

The GSEA-P R and Java programs compute several additional statistics that may be useful to the advanced user:

> ***Tag %***: The percentage of gene tags before (for positive *ES*) or after (for negative *ES*) the peak in the running enrichment score *S*. The larger the percentage, the more tags in the gene set contribute to the final enrichment score.
>
> ***Gene %*:** The percentage of genes in the gene list *L* before (for positive *ES*) or after (for negative *ES*) the peak in the running enrichment score, thus it gives an indication of where in the list the enrichment score is attained.
>
> ***Signal strength**:* The enrichment signal strength that combines the two previous statistics: *(Tag %) x (1 – Gene %) x (N / (N - $N_h$)* , where *N* = the number of genes in the list and $N_h$ is the number of genes in the gene set. The larger this quantity the more enriched the gene set is as a whole. If the gene set is entirely within the first $N_h$ positions in the list, then the *signal strength* is maximal or 1. If the gene set is spread throughout the list, then the signal strength decreases towards 0.
>
> ***FDR (median):*** An additional FDR q-value computed by using a median null distribution. These values are in general more optimistic than the standard FDR q-values as the median null is a representative of the typical random permutation null rather than the extremes. For this reason, we do not recommend it for common use. However, the FDR median is sometimes useful as a binary indicator function (zero vs. non-zero). When it is zero, it indicates that for those extreme

NES values the observed scores are larger than the values obtained by at least half of the random permutations. One advantage of selecting gene sets in this manner (FDR median = 0) is that a predefined threshold is not required. In practice the gene sets selected in this way appear to be roughly the same as those for which the regular FDR is less than 0.25. For example in the Leukemia ALL/AML example the FDR median is zero for the 5 top scoring sets (4 of which have FDR < 0.25).

***glob.p.val****:* A global nominal p-value for each gene set's NES estimated by the % of all ($S, \pi$) with $NES(S, \pi) \geq NES(S)$. Theoretically, for a given level of significance (e.g., 0.05), this quantity measures whether the shift of the tail of the distribution of observed values is extreme enough to declare the observed distribution as different from the null. In principle it allows us to compute a quantitative measure of whether there is any enrichment in the dataset with respect to the given database of gene sets. In practice this quantity behaves in a somewhat noisy way because of the sparseness in the tail of the observed distribution.

- One set of *global reports and plots*. They include the scores and significance estimates for each gene set, the gene list correlation profile, the global observed and null densities and a heat map for the sorted dataset.

- A variable number of specific *gene set reports and plots* (one for each gene set). These include a list of the members of the set and the leading-edge, a gene set running enrichment "mountain" plot, the gene set null distribution and a heat map for genes in the gene set.

The format (columns) for the global result files is as follows.

**GS**: Gene set name.
**SIZE**: Number of genes in the set.
**SOURCE**: Set definition or source.
**ES**: Enrichment score.
**NES**: Normalized (multiplicative rescaling) normalized enrichment score.
**NOM p-val**: Nominal p-value (from the null distribution of the gene set).
**FDR q-val**: False discovery rate q-values.
**FWER p-val**: Family wise error rate p-values.
**Tag %:** Percent of gene set before running enrichment peak.
**Gene %:** Percent of gene list before running enrichment peak.
**Signal**: Enrichment signal strength.
**FDR (median)**: FDR q-values from the median of the null distributions.
**glob.p.val**: P-value using a global statistic (number of sets above the given set's NES).

The rows are sorted by the NES values (from maximum positive or negative NES to minimum).

The format (columns) for the individual gene set result files contains the following information for each gene in the set:

**PROBE_ID**: The gene name or accession number in the dataset.
**SYMBOL**: gene symbol from the gene annotation file.
**DESC**: gene description (title) from the gene annotation file.
**LIST LOC**: location of the gene in the sorted gene list.
**S2N**: signal to noise ratio (correlation) of the gene in the gene list.
**RES**: value of the running enrichment score at the gene location.
**CORE_ENRICHMENT:** Yes or No variable specifying if the gene is in the leading-edge subset.

The rows are sorted by the gene location in the gene list.

## 6 Post GSEA analysis: leading-edge subset similarity, clustering, and assignment.

In analyzing the top scoring gene sets resulting from GSEA we may wish to determine whether their GSEA signal derives from a common subset of genes. This tells us whether we should interpret the sets as representatives of independent processes, or if, in fact, they result from the same common mechanism. If we find that this subset of genes behaves similarly and coherently we may wish to treat it as a new gene set in one of our collections.

In order to make the discovery of such common, overlapping signals with the leading-edge subsets of high-scoring gene sets, we have created software that reads the GSEA results and creates several post-analysis reports and visualizations. The software performs the following three basic types of analyses:

i) Creates a *similarity matrix* heat map that shows at a glance if two gene sets' leading-edge subsets are highly overlapping.

ii) Creates an *assignment matrix* of gene sets vs. leading-edge genes for each phenotype. This binary matrix shows explicitly the membership of each gene in each high-scoring gene set and the overlaps between the gene sets.

iii) Performs a hierarchical clustering (using average linkage) and re-sorts the genes and gene sets in the *assignment matrix* according to their similarity to create *clustered assignment matrices* for each phenotype. This clustering helps to uncover common occurrences of the same leading-edge genes in several gene sets.

As described in the paper we used this program to study the top scoring gene sets enriched in the p53 mutant cancer cell lines (see Figure 3).

This type of analysis helps in the interpretation of GSEA results and the identification of leading-edge overlaps between gene sets that are responsible for high enrichment scores. If applied systematically it can also provide a method for refining genes sets and creating new ones.

## 7 Original GSEA method from Mootha et al. 2003.

Here we described the original GSEA method as defined in Mootha et al. 2003.

> **Step 1: Calculate enrichment.** We set the constant step size of the walk, so that it begins and ends with 0, and the area under the running sum is fixed to account for variations in gene set size. We walk down the list L, incrementing the running sum statistic by $\sqrt{(N - N_h)/N_h}$ when we encounter a gene in S and decrementing by $\sqrt{N_h/(N - N_h)}$ if the gene is not in *S,* where $N$ is the number of genes in the list *L,* and $N_h$ is the number of genes in the gene set *S*. The maximum deviation from zero is the enrichment score (ES) for the gene set S, and corresponds to a standard Kolmogorov-Smirnov statistic (11).
>
> **Step 2: Determine the significance of ES.** We permuted the phenotype labels and re-computed the ES of a gene set to generate a null distribution of ES. Using this null we computed an empirical, nominal P-value for the observed ES.
>
> **Step 3: Adjust for multiple hypothesis testing (MHT).** When scoring multiple gene sets we constructed a null distribution to estimate the family-wise-error rate (FWER) by constructing a histogram of the maximum ES score achieved by any gene set for a given permutation of the phenotype labels. The FWER provides a very conservative correction, which controls the probability of even a single false positive.

Notice that except for the normalization procedure (and the use of FDR instead of FWER) the current GSEA method with p=0 is quite similar to this original GSEA method.

## 8 GSEA-P R program.

> The R scripts and data which produced the results and figures in this paper are available at www.broad.mit.edu/GSEA.

1. Armstrong, S. A., Staunton, J. E., Silverman, L. B., Pieters, R., den Boer, M. L., Minden, M. D., Sallan, S. E., Lander, E. S., Golub, T. R. & Korsmeyer, S. J. (2002) *Nat Genet* **30,** 41-7.

2. Beer, D. G., Kardia, S. L., Huang, C. C., Giordano, T. J., Levin, A. M., Misek, D. E., Lin, L., Chen, G., Gharib, T. G., Thomas, D. G., et al. (2002) *Nat Med* **8,** 816-24.
3. Bhattacharjee, A., Richards, W. G., Staunton, J., Li, C., Monti, S., Vasa, P., Ladd, C., Beheshti, J., Bueno, R., Gillette, M., et al. (2001) *Proc Natl Acad Sci U S A* **98,** 13790-5.
4. Garber, M. E., Troyanskaya, O. G., Schluens, K., Petersen, S., Thaesler, Z., Pacyna-Gengelbach, M., van de Rijn, M., Rosen, G. D., Perou, C. M., Whyte, R. I., et al. (2001) *Proc Natl Acad Sci U S A* **98,** 13784-9.
5. Xie, X., Lu, J., Kulbokas, E. J., Golub, T. R., Mootha, V., Lindblad-Toh, K., Lander, E. S. & Kellis, M. (2005) *Nature* **434,** 338-45.
6. Brentani, H., Caballero, O. L., Camargo, A. A., da Silva, A. M., da Silva, W. A., Jr., Dias Neto, E., Grivet, M., Gruber, A., Guimaraes, P. E., Hide, W., et al. (2003) *Proc Natl Acad Sci U S A* **100,** 13418-23.
7. Su, A. I., Wiltshire, T., Batalov, S., Lapp, H., Ching, K. A., Block, D., Zhang, J., Soden, R., Hayakawa, M., Kreiman, G., et al. (2004) *Proc Natl Acad Sci U S A* **101,** 6062-7.
8. Su, A. I., Welsh, J. B., Sapinoso, L. M., Kern, S. G., Dimitrov, P., Lapp, H., Schultz, P. G., Powell, S. M., Moskaluk, C. A., Frierson, H. F., Jr., et al. (2001) *Cancer Res* **61,** 7388-93.
9. Ramaswamy, S., Tamayo, P., Rifkin, R., Mukherjee, S., Yeang, C. H., Angelo, M., Ladd, C., Reich, M., Latulippe, E., Mesirov, J. P., et al. (2001) *Proc Natl Acad Sci U S A* **98,** 15149-54.
10. von Mises, R. (1964) *Mathematical Theory of Probability and Statistics* (Academic Press, New York).
11. Hollander, M. & Wolfe, D. A. (1999) *Nonparametric statistical methods* (J. Wiley, New York).

Figure SF1A

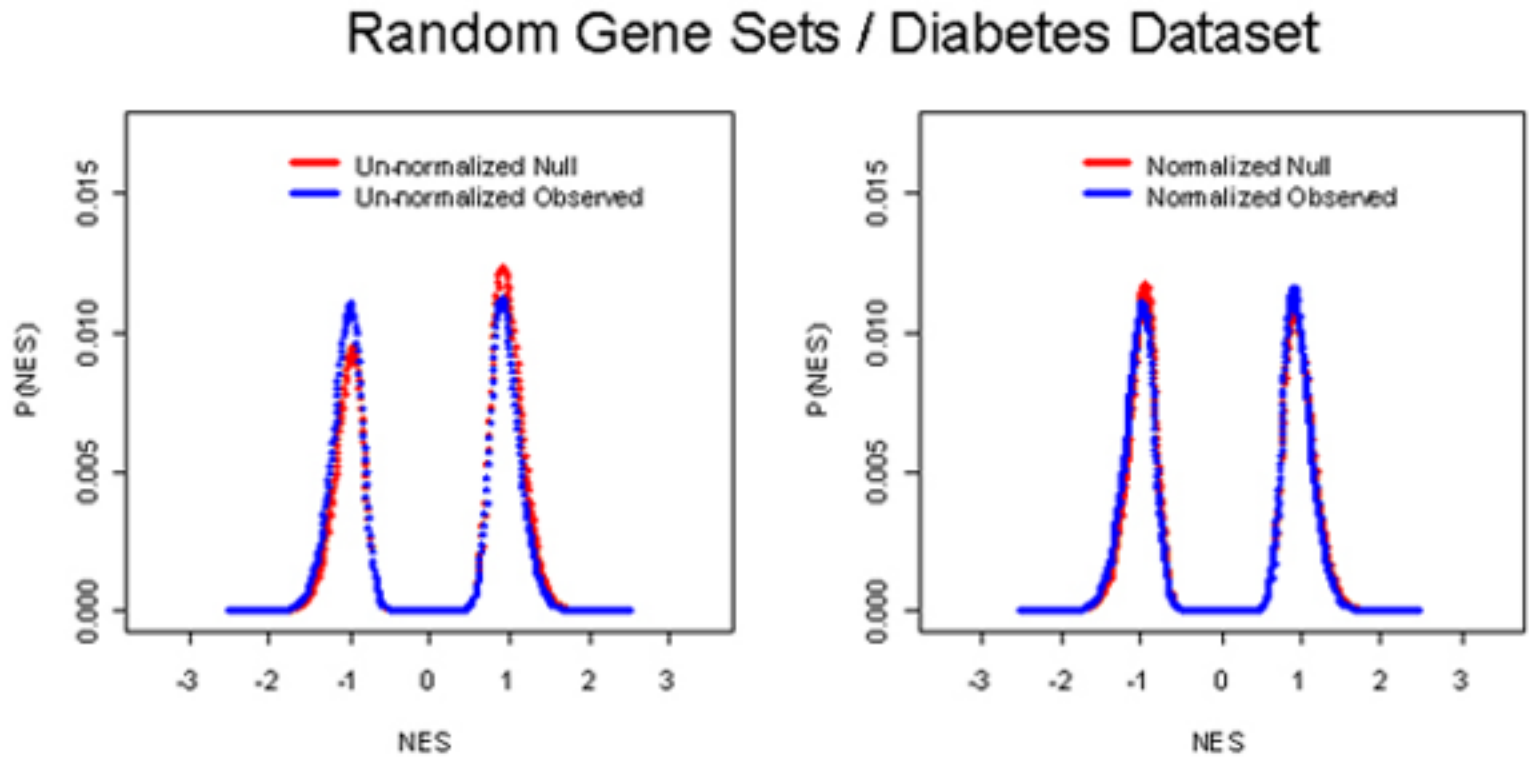


Figure SF1B

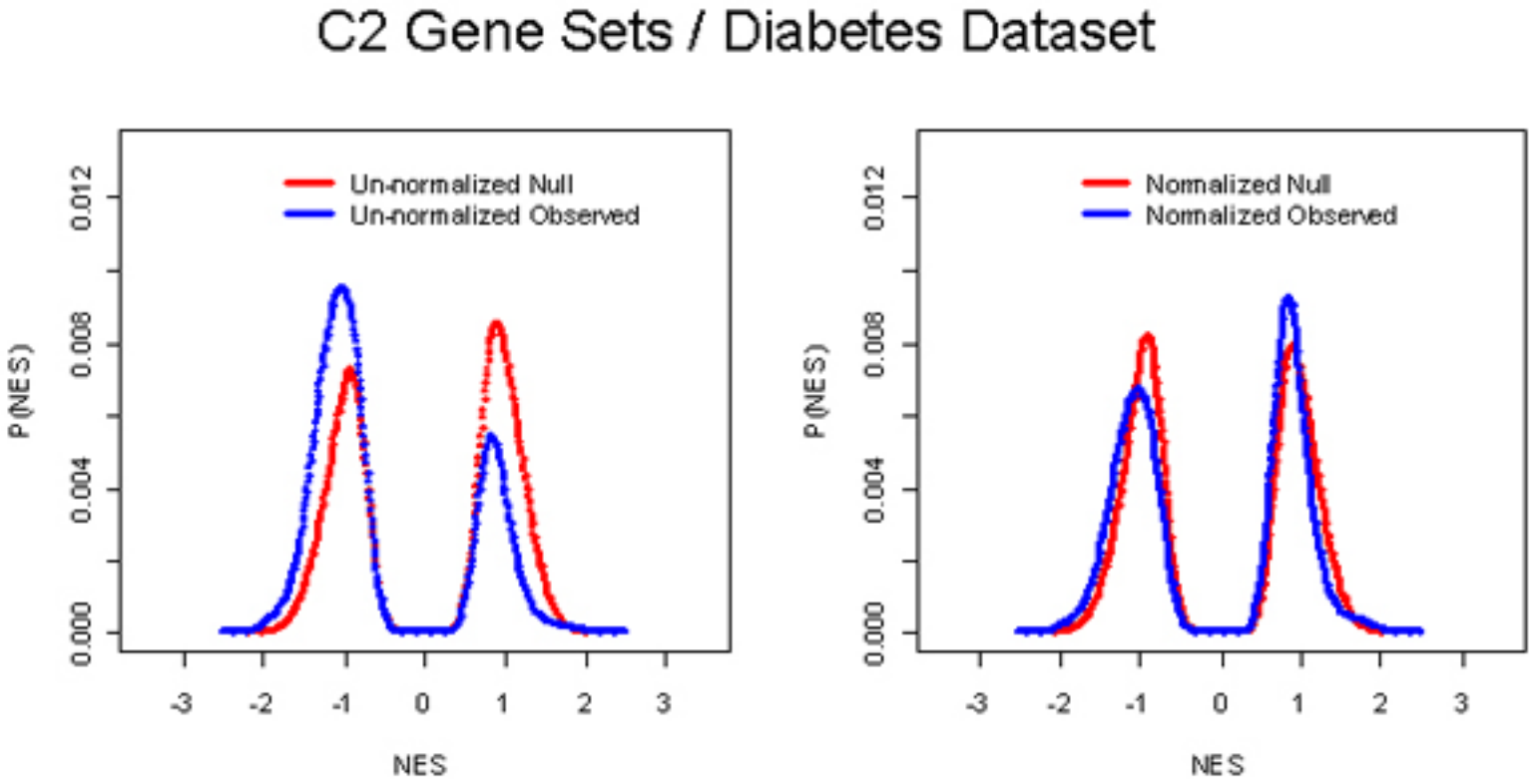

Figure SF1C

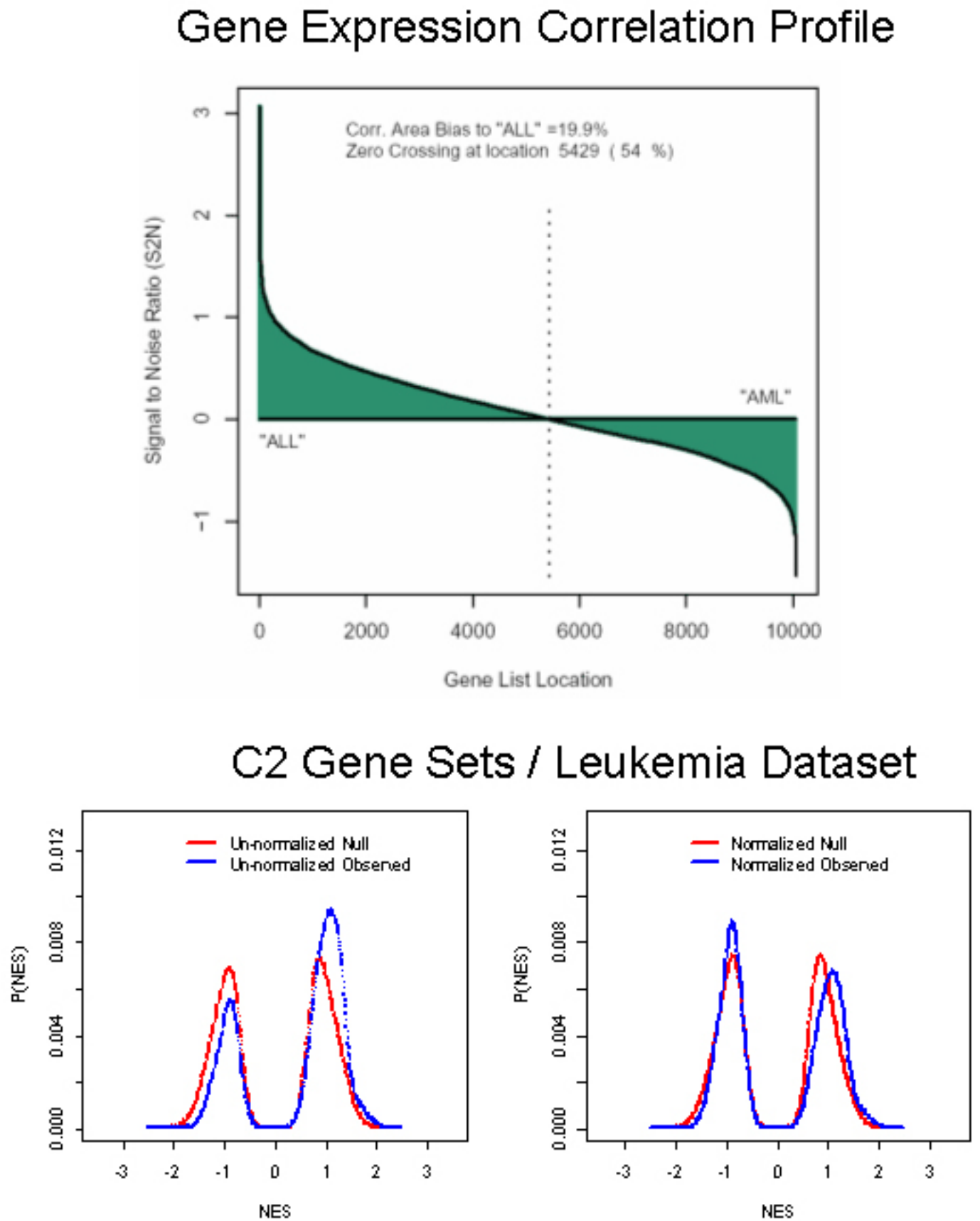
Gene Expression Correlation Profile
Corr. Area Bias to "ALL" =19.9%
Zero Crossing at location 5429 ( 54 %)
Signal to Noise Ratio (S2N)
"AML"
"ALL"
Gene List Location
C2 Gene Sets / Leukemia Dataset
Un-normalized Null
Un-normalized Observed
Normalized Null
Normalized Observed
P(NES)
NES

Figure SF2

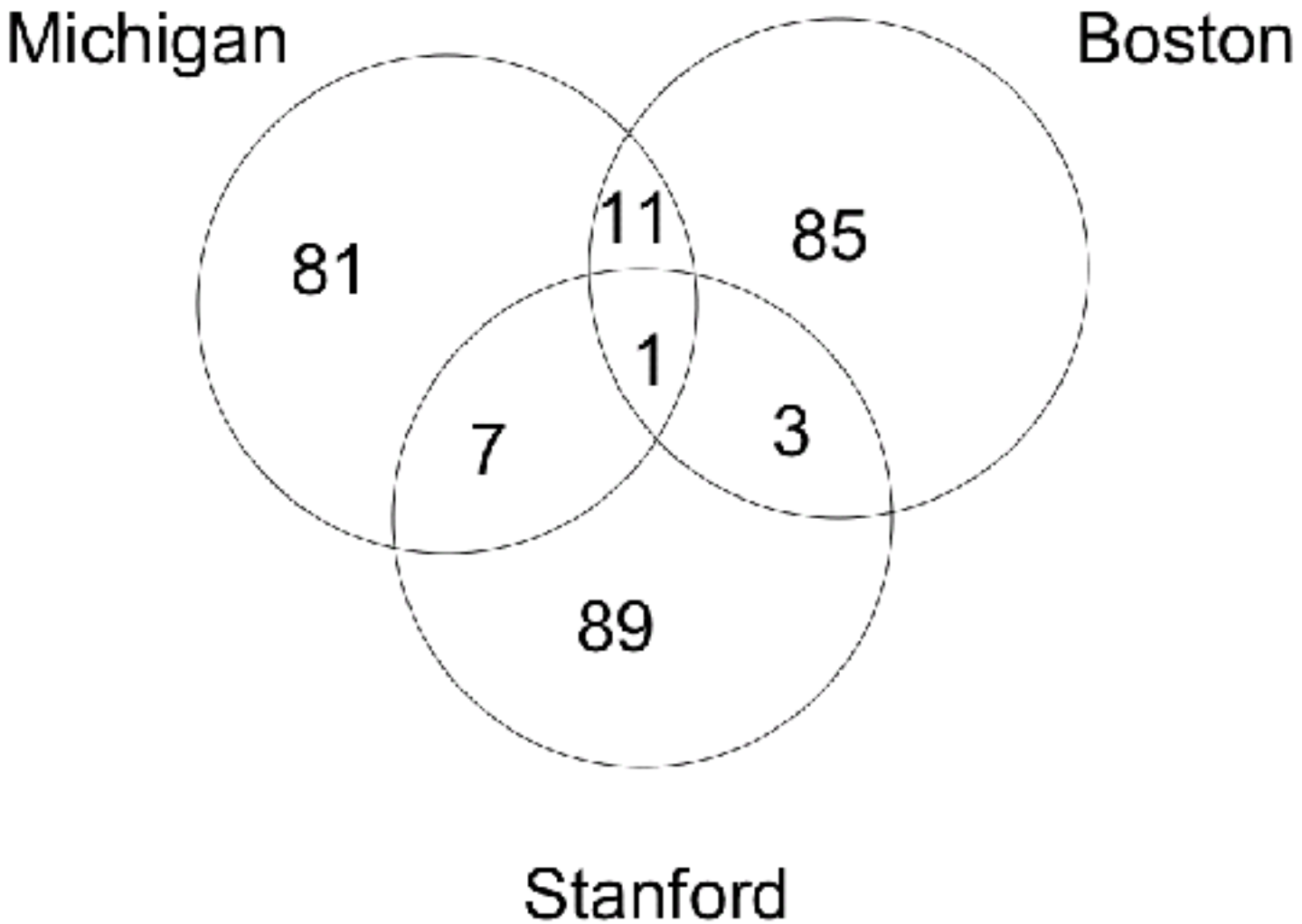

Figure SF3

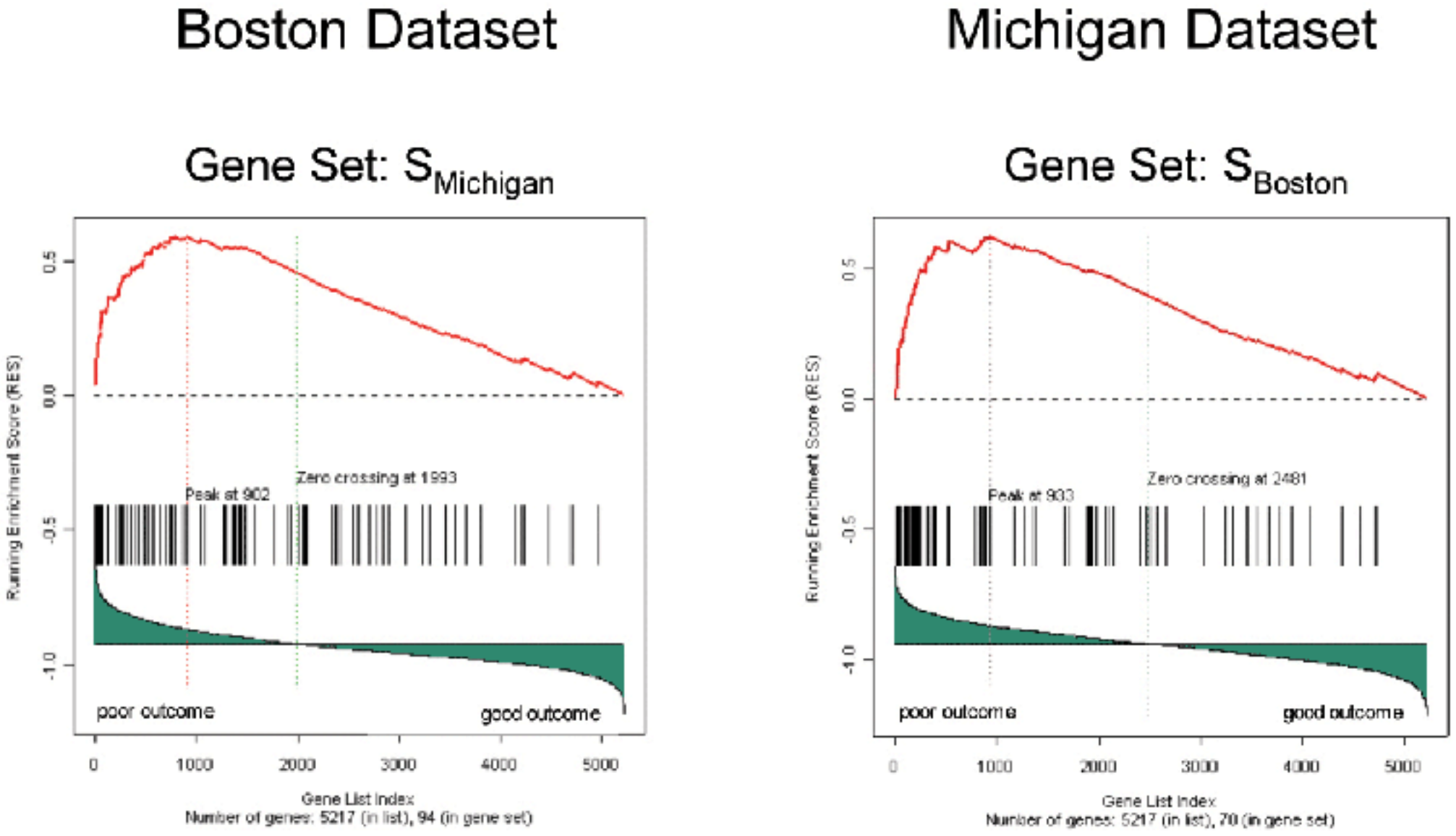
Boston Dataset
Gene Set: S Michigan
Running Enrichment Score (RES)
0.5
0.0
-0.5
-1.0
Peak at 902
Zero crossing at 1993
poor outcome
good outcome
0
1000
2000
3000
4000
5000
Gene List Index
Number of genes: 5217 (in list), 94 (in gene set)
Michigan Dataset
Gene Set: S Boston
Running Enrichment Score (RES)
0.5
0.0
-0.5
-1.0
Peak at 903
Zero crossing at 2481
poor outcome
good outcome
0
1000
2000
3000
4000
5000
Gene List Index
Number of genes: 5217 (in list), 70 (in gene set)

Figure SF4

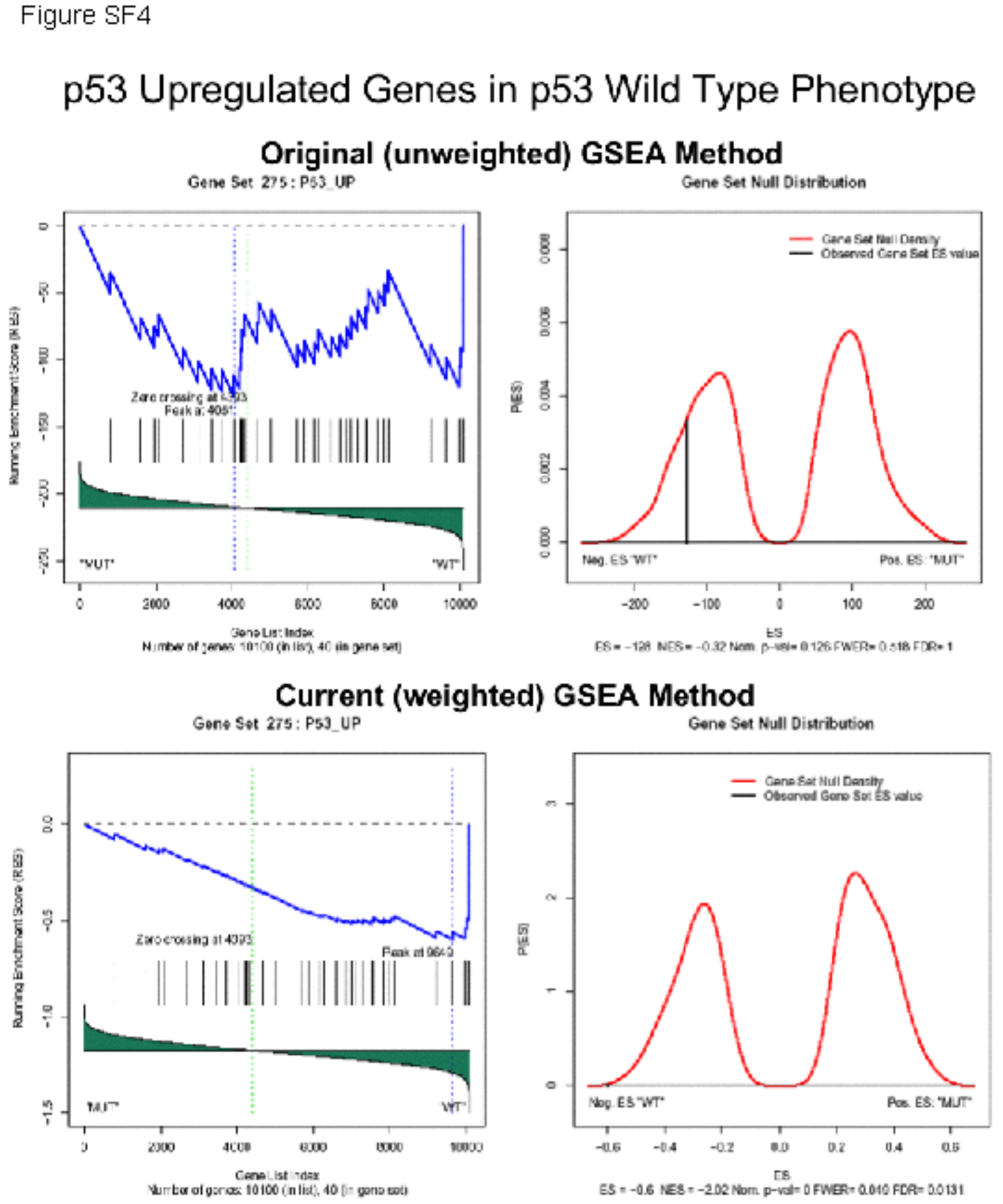
p53 Upregulated Genes in p53 Wild Type Phenotype
Original (unweighted) GSEA Method
Gene Set: 275 : P53_UP
Gene Set Null Distribution
Gene Set Null Density
Observed Gene Set ES value
Running Enrichment Score (RES)
P(ES)
Zero crossing at 4393
Peak at 4057
"MUT"
"WT"
Neg. ES "WT"
Pos. ES "MUT"
Gene List Index
Number of genes: 10100 (in list), 40 (in gene set)
ES
ES = -.128 NES = -0.32 Nom. p-val= 0.126 FWER= 0.518 FDR= 1
Current (weighted) GSEA Method
Gene Set: 275 : P53_UP
Gene Set Null Distribution
Gene Set Null Density
Observed Gene Set ES value
Running Enrichment Score (RES)
P(ES)
Zero crossing at 4393
Peak at 9643
MUT"
WT"
Neg. ES "WT"
Pos. ES: "MUT"
Gene List Index
Number of genes: 10100 (in list), 40 (in gene set)
ES
ES = -0.6 NES = -2.02 Nom. p-val= 0 FWER= 0.010 FDR= 0.0131

Table S1

| DATABASE | TOTAL # OF SETS | # SMALLER THAN 15 | # GREATER THAN 500 | # USED | % USED |
|---|---|---|---|---|---|
| C1 | 319 | 74 | 10 | 235 | 74% |
| C2 | 522 | 194 | 0 | 328 | 63% |
| C3 | 57 | 0 | 0 | 57 | 100% |
| C4 | 427 | 0 | 0 | 427 | 100% |

| GENE SET | SOURCE | ES | NES | NOM p-val | FDR q-val |
|---|---|---|---|---|---|
| **Dataset: Lymphoblast Cell Lines** | | | | | |
| | | | | | |
| **Enriched in Males** | | | | | |
| **chrY** | **C1: Chromosome Y** | **-0.78** | **-2.37** | **<0.001** | **<0.001** |
| **chrYp11** | **C1: Cytogenetic band** | **-0.76** | **-2.14** | **<0.001** | **<0.001** |
| **chrYq11** | **C1: Cytogenetic band** | **-0.89** | **-2.13** | **<0.001** | **<0.001** |
| chr9q21 | C1: Cytogenetic band | -0.43 | -1.53 | 0.035 | 0.630 |
| chr6q24 | C1:Cytogenetic band | -0.53 | -1.44 | 0.086 | 1.000 |
| chr13q13 | C1:Cytogenetic band | -0.45 | -1.40 | 0.090 | 1.000 |
| chr11q22 | C1:Cytogenetic band | -0.44 | -1.39 | 0.094 | 1.000 |
| chr2q32 | C1:Cytogenetic band | -0.46 | -1.33 | 0.139 | 1.000 |
| chr1q24 | C1:Cytogenetic band | -0.39 | -1.31 | 0.111 | 1.000 |
| chr5p13 | C1:Cytogenetic band | -0.40 | -1.31 | 0.150 | 1.000 |
| chr5p15 | C1:Cytogenetic band | -0.37 | -1.26 | 0.154 | 1.000 |
| chr2q24 | C1:Cytogenetic band | -0.44 | -1.26 | 0.238 | 1.000 |
| chr21q22 | C1:Cytogenetic band | -0.31 | -1.25 | 0.150 | 1.000 |
| chr17p11 | C1:Cytogenetic band | -0.37 | -1.24 | 0.172 | 1.000 |
| chr21 | C1: Chromosome Y | -0.30 | -1.24 | 0.164 | 1.000 |
| chr8p12 | C1: Cytogenetic band | -0.37 | -1.23 | 0.165 | 1.000 |
| chr3p25 | C1: Cytogenetic band | -0.36 | -1.23 | 0.201 | 1.000 |
| chr9q34 | C1: Cytogenetic band | -0.30 | -1.21 | 0.211 | 1.000 |
| chr4q13 | C1: Cytogenetic band | -0.39 | -1.20 | 0.245 | 1.000 |
| chr7p21 | C1: Cytogenetic band | -0.41 | -1.19 | 0.262 | 1.000 |
| | | | | | |
| **Testis expressed genes** | **C2: Experimental GNF** | **-0.61** | **-1.99** | **<0.001** | **0.012** |
| Butanoate metabolism | C2: GenMAPP | -0.52 | -1.56 | 0.035 | 1.000 |
| nfkb reduced | C2: Hinata et al 2003 | -0.55 | -1.46 | 0.068 | 1.000 |
| lair pathway | C2: BioCarta | -0.47 | -1.43 | 0.059 | 1.000 |
| Kras upregulated (A549) | C2: Cordero et al 2005 | -0.35 | -1.39 | 0.051 | 1.000 |
| Androgen receptor target genes | C2: Curated from NetAffx | -0.37 | -1.38 | 0.043 | 1.000 |
| Androgen receptor target genes (mouse) | C2: Manually curated | -0.37 | -1.38 | 0.043 | 1.000 |
| shh pathway | C2: BioCarta | -0.49 | -1.38 | 0.090 | 1.000 |
| Wnt Ca2 cyclic GMP pathway | C2: Signalling Transduction KE | -0.48 | -1.37 | 0.127 | 1.000 |
| CD44 ligation upregulated genes | C2: *Hogerkorp et al 2003* | -0.46 | -1.35 | 0.107 | 1.000 |
| Cancer related cell adhesion and motlity genes | C2: Brentani 2003 | -0.33 | -1.32 | 0.103 | 1.000 |
| gata3 pathway | C2: BioCarta | -0.42 | -1.31 | 0.117 | 1.000 |
| Epithelial-mesenchymal transition (EMT) down | C2: Jechlinger et al 2003 | -0.39 | -1.30 | 0.151 | 1.000 |
| Androgen and testosterone target genes | C2: Curated from NetAffx | -0.33 | -1.28 | 0.100 | 1.000 |
| Androgen genes | C2: Netaffx | -0.32 | -1.21 | 0.170 | 1.000 |
| cell adhesion | C2: GO | -0.30 | -1.21 | 0.186 | 1.000 |
| Inflammatory response pathway | C2: BioCarta | -0.38 | -1.20 | 0.243 | 1.000 |
| GPCRs class B secretin-like | C2: GO | -0.40 | -1.20 | 0.241 | 1.000 |
| Cell signal transduction | C2: Signalling Transduction KE | -0.33 | -1.19 | 0.207 | 1.000 |
| inflammatory pathway | C2: BioCarta | -0.38 | -1.19 | 0.226 | 1.000 |
| | | | | | |
| **Enriched in Females** | | | | | |
| chrXp22 | C1: Cytogenetic band | 0.39 | 1.54 | 0.013 | 1.000 |
| chr6q15 | C1: Cytogenetic band | 0.55 | 1.53 | 0.046 | 1.000 |
| chr8q11 | C1: Cytogenetic band | 0.56 | 1.50 | 0.059 | 0.905 |
| chr8p11 | C1: Cytogenetic band | 0.49 | 1.50 | 0.055 | 0.691 |
| chr12q23 | C1: Cytogenetic band | 0.49 | 1.48 | 0.062 | 0.646 |
| chr13q14 | C1: Cytogenetic band | 0.38 | 1.31 | 0.144 | 1.000 |
| chrXq23 | C1: Cytogenetic band | 0.48 | 1.29 | 0.175 | 1.000 |
| chr10q11 | C1: Cytogenetic band | 0.37 | 1.26 | 0.168 | 1.000 |
| chr2q31 | C1: Cytogenetic band | 0.35 | 1.26 | 0.156 | 1.000 |
| chr4q22 | C1: Cytogenetic band | 0.45 | 1.24 | 0.195 | 1.000 |
| chrXp11 | C1: Cytogenetic band | 0.31 | 1.23 | 0.149 | 1.000 |
| chr3q29 | C1: Cytogenetic band | 0.43 | 1.23 | 0.219 | 1.000 |
| chr8p23 | C1: Cytogenetic band | 0.38 | 1.17 | 0.251 | 1.000 |
| chr20p12 | C1: Cytogenetic band | 0.34 | 1.16 | 0.257 | 1.000 |
| chr16p12 | C1: Cytogenetic band | 0.35 | 1.10 | 0.317 | 1.000 |
| chr1p34 | C1: Cytogenetic band | 0.28 | 1.06 | 0.400 | 1.000 |
| chr13q12 | C1: Cytogenetic band | 0.30 | 1.04 | 0.405 | 1.000 |
| chr2q14 | C1: Cytogenetic band | 0.33 | 1.04 | 0.411 | 1.000 |
| chr5q14 | C1: Cytogenetic band | 0.34 | 1.04 | 0.396 | 1.000 |
| chr11p11 | C1: Cytogenetic band | 0.31 | 1.04 | 0.409 | 1.000 |

| | | | | | |
|---|---|---|---|---|---|
| **X inactivation genes** | **C2: *Willard et al 1999 & Disteche et al 2002*** | **0.80** | **2.29** | **<0.001** | **<0.001** |
| **Female reproductive tissue expressed genes** | **C2: Experimental GNF** | **0.48** | **1.89** | **0.013** | **0.045** |
| Cell cycle arrest | C2: GO | 0.54 | 1.66 | 0.015 | 0.557 |
| tel pathway | C2: BioCarta | 0.58 | 1.61 | 0.023 | 0.643 |
| Insulin upregulated | C2: Rome et al 2003 | 0.48 | 1.61 | 0.030 | 0.546 |
| mRNA splicing | C2: BioCarta | 0.60 | 1.56 | 0.056 | 0.657 |
| Proteasome degradation | C2: BioCarta | 0.64 | 1.52 | 0.095 | 0.776 |
| Leucine deprivation downregulated genes | C2: Peng et al 2002 | 0.54 | 1.52 | 0.109 | 0.717 |
| Rapamycin downregulated genes | C2: *Peng et al 2002* | 0.52 | 1.50 | 0.127 | 0.699 |
| Proteasome pathway | C2: BioCarta | 0.68 | 1.48 | 0.093 | 0.739 |
| Dictyostelium discoideum cAMP chemotaxis pathway | C2: Signalling Transduction KE | 0.46 | 1.47 | 0.066 | 0.750 |
| Glutamine deprivation downregulated genes | C2: Peng et al 2002 | 0.48 | 1.44 | 0.166 | 0.832 |
| mRNA processing | C2: BioCarta | 0.55 | 1.42 | 0.159 | 0.879 |
| G1 and S phases | C2: SigmaAldrich | 0.51 | 1.37 | 0.121 | 1.000 |
| rho pathway | C2: BioCarta | 0.45 | 1.36 | 0.152 | 1.000 |
| mtor pathway | C2: BioCarta | 0.52 | 1.36 | 0.149 | 1.000 |
| Cell cycle pathway | C2: BioCarta | 0.51 | 1.34 | 0.160 | 1.000 |
| raccycd pathway | C2: BioCarta | 0.50 | 1.30 | 0.236 | 1.000 |
| TCA tricarboxylic acid cycle | C2: Manually Curated | 0.61 | 1.29 | 0.234 | 1.000 |
| ATP synthesis | C2: GenMAPP | 0.44 | 1.27 | 0.204 | 1.000 |

| GENE SET | SOURCE | ES | NES | NOM p-val | FDR q-val |
|---|---|---|---|---|---|
| **Dataset: p53 status in NCI-60 Cell Lines** | | | | | |
| | | | | | |
| **Enriched in p53 Mutant** | | | | | |
| **Ras signaling pathway** | **C2: BioCarta** | **0.60** | **1.89** | **0.002** | **0.171** |
| ngf pathway | C2: BioCarta | 0.59 | 1.79 | 0.002 | 0.295 |
| Upregulated by hoxa9 | C2: Manually Curated | 0.58 | 1.76 | 0.011 | 0.275 |
| igf1 pathway | C2: BioCarta | 0.56 | 1.74 | 0.008 | 0.257 |
| X_inactivation genes | C2: Willard et al 1999 & Disteche et al 2002 | 0.61 | 1.65 | 0.035 | 0.487 |
| egf pathway | C2: BioCarta | 0.48 | 1.60 | 0.024 | 0.609 |
| insulin pathway | C2: BioCarta | 0.49 | 1.56 | 0.023 | 0.697 |
| MAPK cascade | C2: GO | 0.49 | 1.55 | 0.016 | 0.648 |
| BRCA upregulated | C2: Welcsh_et_al_2002 | 0.46 | 1.55 | 0.036 | 0.599 |
| wrk1, erk2, mapk pathway | C2: Signalling Transduction KE | 0.44 | 1.55 | 0.024 | 0.541 |
| nfkb reduced | C2: Hinata et al 2003 | 0.58 | 1.52 | 0.051 | 0.600 |
| gcr pathway | C2: BioCarta | 0.50 | 1.50 | 0.053 | 0.635 |
| pitx2 pathway | C2: BioCarta | 0.52 | 1.48 | 0.069 | 0.687 |
| erk pathway | C2: BioCarta | 0.44 | 1.47 | 0.046 | 0.652 |
| B cell receptor complexes | SigmaAldrich | 0.45 | 1.47 | 0.044 | 0.622 |
| bcr pathway | C2: BioCarta | 0.43 | 1.46 | 0.035 | 0.609 |
| pdgf pathway | C2: BioCarta | 0.45 | 1.45 | 0.075 | 0.606 |
| Phosphoinositide 3 kinase pathway | C2: Signalling Transduction KE | 0.40 | 1.45 | 0.046 | 0.584 |
| Proteasome pathway | C2: BioCarta | 0.55 | 1.45 | 0.121 | 0.561 |
| fmlp pathway | C2: BioCarta | 0.38 | 1.40 | 0.063 | 0.710 |
| | | | | | |
| **Enriched in p53 Wild Type** | | | | | |
| **Hypoxia and p53 in the Cardiovascular system** | **C2: BioCarta** | **-0.68** | **-2.21** | **<0.001** | **<0.001** |
| **Stress induction of HSP regulation** | **C2: BioCarta** | **-0.78** | **-2.20** | **<0.001** | **<0.001** |
| **p53 signaling pathway** | **C2: BioCarta** | **-0.75** | **-2.18** | **<0.001** | **<0.001** |
| **p53 upregulated genes** | **C2: *Kannan et al 2001*** | **-0.60** | **-2.02** | **<0.001** | **0.013** |
| **Radiation sensitivity genes** | **C2: BioCarta** | **-0.57** | **-1.86** | **0.002** | **0.078** |
| ck1 pathway | C2: BioCarta | -0.54 | -1.64 | 0.027 | 0.495 |
| inflammatory pathway | C2: BioCarta | -0.54 | -1.62 | 0.029 | 0.477 |
| no2il12 pathway | C2: BioCarta | -0.63 | -1.62 | 0.041 | 0.434 |
| GPCRs Class A Rhodopsin-like | C2: GO | -0.43 | -1.55 | 0.040 | 0.608 |
| bad pathway | C2: BioCarta | -0.47 | -1.54 | 0.044 | 0.575 |
| Cytokine pathway | C2: BioCarta | -0.54 | -1.54 | 0.055 | 0.539 |
| lair pathway | C2: BioCarta | -0.57 | -1.53 | 0.048 | 0.510 |
| p53 signalling | C2: BioCarta | -0.34 | -1.52 | 0.013 | 0.513 |
| Chemical pathway | C2: BioCarta | -0.46 | -1.50 | 0.044 | 0.534 |
| Glycerolipid_metabolism | C2: GenMAPP | -0.42 | -1.48 | 0.048 | 0.567 |
| Interleukin 4 pathway | C2: Signalling Transduction KE | -0.40 | -1.39 | 0.076 | 0.848 |
| Photosynthesis | C2: GenMAPP | -0.56 | -1.39 | 0.164 | 0.814 |
| nkt pathway | C2: BioCarta | -0.43 | -1.38 | 0.124 | 0.798 |
| Cell adhesion receptor activity | C2: GO | -0.40 | -1.37 | 0.081 | 0.769 |

| | | | | | |
|---|---|---|---|---|---|
| Telomerase downregulated genes | C2: Smith et al 2003 | -0.34 | -1.35 | 0.093 | 0.842 |

| GENE SET | SOURCE | ES | NES | NOM p-val | FDR q-val |
|---|---|---|---|---|---|
| **Dataset: Acute Leukemias** | | | | | |
| | | | | | |
| **Enriched in ALL** | | | | | |
| **chr6q21** | **C1: Cytogenetic band** | **0.66** | **2.07** | **<0.001** | **0.011** |
| **chr5q31** | **C1: Cytogenetic band** | **0.50** | **1.91** | **<0.001** | **0.046** |
| **chr13q14** | **C1: Cytogenetic band** | **0.57** | **1.87** | **<0.001** | **0.057** |
| **chr14q32** | **C1: Cytogenetic band** | **0.47** | **1.81** | **0.006** | **0.082** |
| **chr17q23** | **C1: Cytogenetic band** | **0.53** | **1.81** | **0.017** | **0.071** |
| chr1q42 | C1: Cytogenetic band | 0.49 | 1.61 | 0.057 | 0.355 |
| chr6 | C1: Chromosome 6 | 0.32 | 1.59 | 0.017 | 0.354 |
| chr10q24 | C1: Cytogenetic band | 0.45 | 1.58 | 0.010 | 0.319 |
| chr3q13 | C1: Cytogenetic band | 0.46 | 1.54 | 0.024 | 0.391 |
| chr10p15 | C1: Cytogenetic band | 0.49 | 1.49 | 0.052 | 0.470 |
| chr13 | C1: Chromosome 13 | 0.34 | 1.47 | 0.039 | 0.492 |
| chr6p21 | C1: Cytogenetic band | 0.35 | 1.46 | 0.092 | 0.483 |
| chr6p22 | C1: Cytogenetic band | 0.37 | 1.44 | 0.100 | 0.504 |
| chr4p16 | C1: Cytogenetic band | 0.38 | 1.43 | 0.075 | 0.512 |
| chr14 | C1: Chromosome 14 | 0.31 | 1.42 | 0.069 | 0.508 |
| chr1q25 | C1: Cytogenetic band | 0.43 | 1.41 | 0.083 | 0.489 |
| chr6q23 | C1: Cytogenetic band | 0.46 | 1.41 | 0.097 | 0.472 |
| chr10q25 | C1: Cytogenetic band | 0.50 | 1.40 | 0.096 | 0.458 |
| chr8p11 | C1: Cytogenetic band | 0.45 | 1.40 | 0.090 | 0.437 |
| chr17q24 | C1: Cytogenetic band | 0.46 | 1.40 | 0.095 | 0.417 |
| | | | | | |
| **Enriched in AML** | | | | | |
| chr15q25 | C1: Cytogenetic band | -0.43 | -1.47 | 0.042 | 1.000 |
| chr1q24 | C1: Cytogenetic band | -0.42 | -1.43 | 0.067 | 1.000 |
| chr7q36 | C1: Cytogenetic band | -0.40 | -1.29 | 0.189 | 1.000 |
| chr17q25 | C1: Cytogenetic band | -0.31 | -1.25 | 0.150 | 1.000 |
| chr7q34 | C1: Cytogenetic band | -0.41 | -1.23 | 0.208 | 1.000 |
| chr19p13 | C1: Cytogenetic band | -0.28 | -1.23 | 0.213 | 1.000 |
| chr4q13 | C1: Cytogenetic band | -0.34 | -1.22 | 0.200 | 1.000 |
| chr15q22 | C1: Cytogenetic band | -0.38 | -1.22 | 0.217 | 1.000 |
| chr2q35 | C1: Cytogenetic band | -0.35 | -1.22 | 0.220 | 1.000 |
| chr16p11 | C1: Cytogenetic band | -0.36 | -1.19 | 0.284 | 1.000 |
| chr12p13 | C1: Cytogenetic band | -0.28 | -1.15 | 0.254 | 1.000 |
| chr20p11 | C1: Cytogenetic band | -0.37 | -1.13 | 0.288 | 1.000 |
| chr19q13 | C1: Cytogenetic band | -0.25 | -1.11 | 0.324 | 1.000 |
| chr1p36 | C1: Cytogenetic band | -0.24 | -1.07 | 0.357 | 1.000 |
| chr19 | C1: Chromosome 19 | -0.23 | -1.07 | 0.376 | 1.000 |
| chr11q24 | C1: Cytogenetic band | -0.32 | -1.05 | 0.401 | 1.000 |
| chr18p11 | C1: Cytogenetic band | -0.30 | -1.04 | 0.394 | 1.000 |
| chr2p13 | C1: Cytogenetic band | -0.30 | -1.03 | 0.418 | 1.000 |
| chr11q12 | C1: Cytogenetic band | -0.25 | -0.99 | 0.475 | 1.000 |
| chr15q26 | C1: Cytogenetic band | -0.30 | -0.98 | 0.508 | 1.000 |

| GENE SET | SOURCE | ES | NES | NOM p-val | FDR q-val |
|---|---|---|---|---|---|
| **Dataset: Lung Cancer Outcome, Boston Study** | | | | | |
| | | | | | |
| **Top 20 Poor Outcome Gene Sets** | | | | | |
| **Hypoxia and p53 in the Cardiovascular system** | **C2: BioCarta** | **-0.67** | **-2.03** | **0.000** | **0.050** |
| **Aminoacyl tRNA biosynthesis** | **C2: GenMAPP** | **-0.77** | **-1.88** | **0.008** | **0.144** |
| **Insulin upregulated genes** | **C2: *Rome et al 2003*** | **-0.51** | **-1.86** | **0.002** | **0.118** |
| **tRNA synthetases** | **C2: BioCarta** | **-0.75** | **-1.80** | **0.010** | **0.157** |
| **Leucine deprivation downregulated genes** | **C2: *Peng et al 2002*** | **-0.58** | **-1.78** | **0.026** | **0.144** |
| **Telomerase upregulated genes** | **C2: *Smith et al 2003*** | **-0.44** | **-1.77** | **0.004** | **0.128** |
| **Glutamine deprivation downregulated genes** | **C2: *Peng et al 2002*** | **-0.51** | **-1.74** | **0.024** | **0.146** |
| **Cell cycle checkpoint** | **C2: GO** | **-0.57** | **-1.67** | **0.013** | **0.216** |
| Proteasome pathway | C2: BioCarta | -0.69 | -1.63 | 0.052 | 0.262 |
| Proteasome degradation | C2: BioCarta | -0.58 | -1.56 | 0.079 | 0.360 |
| Rapamycin downregulated genes | C2: *Peng et al 2002* | -0.44 | -1.51 | 0.087 | 0.450 |
| p53 signalling | C2: BioCarta | -0.40 | -1.47 | 0.035 | 0.526 |
| Kras upregulated (A549) | C2: *Sweet-Cordero et al 2005* | -0.42 | -1.47 | 0.061 | 0.493 |
| Epithelial-mesenchymal transition (EMT) | C2: *Jechlinger et al 2003* | -0.45 | -1.46 | 0.094 | 0.482 |

| | | | | | |
|---|---|---|---|---|---|
| Cell cycle (GO) | C2: GO | -0.45 | -1.41 | 0.137 | 0.591 |
| Starch and sucrose metabolism | C2: GenMAPP | -0.47 | -1.40 | 0.112 | 0.570 |
| Transport of vesicles | C2: *Brentani 2003* | -0.45 | -1.40 | 0.098 | 0.542 |
| Glucose deprivation downregulated genes | C2: *Peng et al 2002* | -0.37 | -1.37 | 0.137 | 0.586 |
| vegf pathway | C2: BioCarta | -0.45 | -1.37 | 0.098 | 0.575 |
| Glycolysis | C2: Manually Curated | -0.49 | -1.36 | 0.146 | 0.549 |

| GENE SET | SOURCE | ES | NES | NOM p-val | FDR q-val |
|---|---|---|---|---|---|
| **Dataset: Lung Cancer Outcome, Michigan Study** | | | | | |
| | | | | | |
| **Top 20 Poor Outcome Gene Sets** | | | | | |
| **Glycolysis Gluconeogenesis** | **C2: GenMAPP** | **-0.61** | **-2.13** | **<0.001** | **0.006** |
| **vegf pathway** | **C2: BioCarta** | **-0.67** | **-2.01** | **<0.001** | **0.028** |
| **Insulin upregulated genes** | **C2: *Rome et al 2003*** | **-0.53** | **-1.88** | **0.004** | **0.147** |
| **Insulin signalling** | **C2: BioCarta** | **-0.41** | **-1.83** | **<0.001** | **0.170** |
| **Telomerase upregulated genes** | **C2: *Smith et al 2003*** | **-0.50** | **-1.80** | **0.006** | **0.188** |
| **Glutamate metabolism** | **C2: GenMAPP** | **-0.62** | **-1.77** | **0.011** | **0.200** |
| **Ceramide pathway** | **C2: BioCarta** | **-0.57** | **-1.75** | **0.004** | **0.204** |
| **p53 signalling** | **C2: BioCarta** | **-0.44** | **-1.75** | **<0.001** | **0.179** |
| **tRNA synthetases** | **C2: BioCarta** | **-0.67** | **-1.70** | **0.025** | **0.225** |
| **Breast cancer estrogen signalling** | **C2: GEArray** | **-0.40** | **-1.68** | **0.008** | **0.250** |
| **Aminoacyl tRNA biosynthesis** | **C2: GenMAPP** | **-0.66** | **-1.68** | **0.024** | **0.229** |
| raccycd pathway | C2: BioCarta | -0.53 | -1.64 | 0.018 | 0.291 |
| cxcr4 pathway | C2: BioCarta | -0.54 | -1.63 | 0.008 | 0.284 |
| mtor pathway | C2: BioCarta | -0.55 | -1.59 | 0.042 | 0.338 |
| bcl2 family and reg. network | C2: GEArray | -0.51 | -1.59 | 0.044 | 0.329 |
| Glucose metabolism | C2: Manually Curated | -0.53 | -1.57 | 0.052 | 0.339 |
| Transport of vesicles | C2: *Brentani 2003* | -0.49 | -1.55 | 0.056 | 0.381 |
| sppa pathway | C2: BioCarta | -0.52 | -1.52 | 0.048 | 0.424 |
| Leucine deprivation downregulated genes | C2: *Peng et al 2002* | -0.48 | -1.52 | 0.104 | 0.417 |
| Glycolysis | C2: Manually Curated | -0.56 | -1.50 | 0.067 | 0.423 |

| GENE SET | SOURCE | ES | NES | NOM p-val | FDR q-val |
|---|---|---|---|---|---|
| **Dataset: Lung Cancer Outcome, Stanford Study** | | | | | |
| | | | | | |
| **Top 20 Poor Outcome Gene Sets** | | | | | |
| Pyrimidine metabolism | C2: GenMAPP | -0.49 | -1.45 | 0.073 | 1.000 |
| Purine metabolism | C2: GenMAPP | -0.40 | -1.38 | 0.084 | 1.000 |
| DNA repair | C2: *Brentani 2003* | -0.47 | -1.33 | 0.152 | 1.000 |
| Kras upregulated (A549) | C2: *Sweet-Cordero et al 2005* | -0.35 | -1.26 | 0.140 | 1.000 |
| Hox regulated genes | C2: Manually Curated | -0.38 | -1.22 | 0.208 | 1.000 |
| ER upregulated genes | C2: *Frasor et al 2004* | -0.42 | -1.22 | 0.233 | 1.000 |
| Fatty acid metabolism | C2: GenMAPP | -0.37 | -1.21 | 0.203 | 1.000 |
| CD44 ligation upregulated genes | C2: *Hogerkorp et al 2003* | -0.40 | -1.15 | 0.299 | 1.000 |
| Caspase pathway | C2: BioCarta | -0.39 | -1.10 | 0.331 | 1.000 |
| Androgen genes | C2: Manually Curated | -0.31 | -1.10 | 0.311 | 1.000 |
| Mitochondrial genes | C2: Manually Curated | -0.28 | -1.07 | 0.402 | 1.000 |
| Human mitocondrial | C2: Manually Curated | -0.29 | -1.06 | 0.425 | 1.000 |
| Cell cycle | C2: *Brentani 2003* | -0.33 | -1.05 | 0.421 | 1.000 |
| Propanoate metabolism | C2: GenMAPP | -0.36 | -1.03 | 0.432 | 1.000 |
| Rapamycin downregulated genes | C2: *Peng et al 2002* | -0.30 | -1.02 | 0.448 | 1.000 |
| Cell cycle (GO) | C2: GO | -0.34 | -1.02 | 0.431 | 1.000 |
| Valine leucine and isoleucine degradation | C2: GenMAPP | -0.37 | -1.01 | 0.449 | 1.000 |
| Mitochondrion (GO 0005739) | C2: GO | -0.28 | -1.01 | 0.445 | 1.000 |
| Electron transport | C2: BioCarta | -0.27 | -0.98 | 0.470 | 1.000 |
| Proteasome degradation | C2: BioCarta | -0.36 | -0.97 | 0.497 | 1.000 |

Table S3

| GENE SET | SOURCE | ES | NES | NOM p-val | FDR q-val |
|---|---|---|---|---|---|
| Dataset: Lymphoblast Cell Lines | | | | | |
| | | | | | |
| Enriched in Males | | | | | |
| C2:Testis expressed autosomal genes | Experimental GNF | 0.559 | 1.724 | 0.001 | 0.181 |
| | | | | | |
| Enriched in Females | | | | | |
| C2:Female reproductive tissue expressed autosomal genes | Experimental GNF | -0.457 | -1.830 | 0.004 | 0.163 |

Table S4

## Lung Outcome Studies – Single Gene Overlaps

| Michigan / Boston (12) | Michigan / Stanford (8) | Stanford / Boston (4) |
|---|---|---|
| **KRT7** | **KRT7** | **KRT7** |
| BZW1 | CSNK1E | CASP4 |
| CASP4 | GALNT3 | GOSR1 |
| CSNK1E | HIP2 | PAICS |
| ENO2 | ITGA2 | |
| FADD | NP | |
| KRT18 | NPAS2 | |
| KRT19 | PAICS | |
| LAMB3 | | |
| P4HA1 | | |
| PFKP | | |
| TUBA1 | | |

| Gene Set | Dataset(s) | Rank(s) in List | Pathway | Process/Context | Major Response/Theme |
|---|---|---|---|---|---|
| | | | | | |
| **Telomerase upregulated genes** | Michigan, Boston | 5, 6 | Telomerase | Telomerase | Telomerase |
| | | | | | |
| | | | | | |
| **Cell cycle (GO)** | Boston, Stanford | 15, 16 | Cell Proliferation | Cell Proliferation | rapid cell proliferation |
| **Cell cycle checkpoint** | Boston | 8 | Cell Proliferation | Cell Proliferation | rapid cell proliferation |
| **Cell cycle** | Stanford | 13 | Cell Proliferation | Cell Proliferation | rapid cell proliferation |
| | | | | | |
| **vegf pathway** | Michigan, Boston | 2, 19 | vegf Signaling | Angiogenesis | rapid cell proliferation |
| | | | | | |
| **Glycolysis** | Michigan, Boston | 20, 20 | Glycolisis | Glycolysis | rapid cell proliferation |
| **Glycolysis Gluconeogenesis** | Michigan | 1 | Glycolysis | Glycoyisis | rapid cell proliferation |
| | | | | | |
| **Glucose metabolism** | Michigan | 16 | Glucose Metabolism | Carbohydrate Metabolism | rapid cell proliferation |
| **Glucose deprivation downregulated genes** | Boston | 18 | Glucose Metabolism | Carbohydrate Metabolism | rapid cell proliferation |
| **Starch and sucrose metabolism** | Boston | 16 | Starch And Sucrose Metabolism | Carbohydrate Metabolism | rapid cell proliferation |
| **Propanoate metabolism** | Stanford | 14 | Propanoate Metabolism | Carbohydrate Metabolism | rapid cell proliferation |
| | | | | | |
| **Insulin upregulated genes** | Michigan, Boston | 3, 3 | Insulin Up Regulated | Insulin Signaling | rapid cell proliferation |
| **Insulin signalling** | Michigan | 4 | Insulin Signaling | Insulin Signaling | rapid cell proliferation |
| | | | | | |
| **Proteasome degradation** | Boston, Stanford | 10, 20 | Proteasome Degradation | Protein Degradation | rapid cell proliferation |
| **Proteasome pathway** | Boston | 9 | Proteasome Pathway | Protein Degradation | rapid cell proliferation |
| | | | | | |
| **Kras upregulated (A549)** | Boston, Stanford | 13, 4 | Ras Signaling | Ras/MAPK Signaling | rapid cell proliferation |
| **raccycd pathway** | Michigan | 12 | Ras Signaling | Ras/MAPK Signaling | rapid cell proliferation |
| | | | | | |
| **Ceramide pathway** | Michigan | 7 | Ceramide Signaling | Ceramide Signaling | rapid cell proliferation |
| | | | | | |
| | | | | | |
| **Glutamine deprivation downregulated genes** | Boston | 7 | Glutamine Metabolism | Amino Acid Metabolism | Rapamycin/Biosynthesis |
| **Leucine deprivation downregulated genes** | Michigan, Boston | 19, 5 | Leucine Starvation Down Regulated | Amino Acid Metabolism | Rapamycin/Biosynthesis |
| **Glutamate metabolism** | Michigan | 6 | Glutamate Metabolism | Amino Acid Metabolism | Rapamycin/Biosynthesis |
| **Valine leucine and isoleucine degradation** | Stanford | 17 | Valine, Isoleucine Degradation | Amino Acid Metabolism | Rapamycin/Biosynthesis |
| **Aminoacyl tRNA biosynthesis** | Michigan, Boston | 11, 2 | tRNA Synthesis | Amino Acid Metabolism | Rapamycin/Biosynthesis |
| **tRNA synthetases** | Michigan, Boston | 9, 4 | tRNA Synthesis | Amino Acid Metabolism | Rapamycin/Biosynthesis |
| | | | | | |
| **Fatty acid metabolism** | Stanford | 7 | Fatif Acid Metabolism | Fatif Acid Metabolism | Rapamycin/Biosynthesis |
| | | | | | |
| **Purine metabolism** | Stanford | 2 | Purine Metabolism | Nucleotide Metabolism | Rapamycin/Biosynthesis |
| **Pyrimidine metabolism** | Stanford | 1 | Pyrimidine Metabolism | Nucleotide Metabolism | Rapamycin/Biosynthesis |
| | | | | | |
| **CD44 ligation upregulated genes** | Stanford | 8 | Chemokine Signaling | Immune Modulation | Rapamycin/Biosynthesis |
| **cxcr4 pathway** | Michigan | 13 | Chemokine Signaling | Immune Modulation | Rapamycin/Biosynthesis |
| | | | | | |
| **mtor pathway** | Michigan | 14 | mTOR Signaling | mTOR Signaling | Rapamycin/Biosynthesis |
| **Rapamycin downregulated genes** | Boston, Stanford | 11, 15 | mTOR Signaling | mTOR Signaling | Rapamycin/Biosynthesis |
| | | | | | |
| **Androgen genes** | Stanford | 10 | Androgen | Androgen Signaling | -- |
| | | | | | |

| | | | | | |
|---|---|---|---|---|---|
| **DNA repair** | Stanford | 3 | DNA Repair | DNA Repair | -- |
| | | | | | |
| **Breast cancer estrogen signalling** | Michigan | 10 | Estrogen Signaling | Estrogen Signaling | -- |
| **ER upregulated genes** | Stanford | 6 | Estrogen Signaling | Estrogen Signaling | -- |
| | | | | | |
| **Hox regulated genes** | Stanford | 5 | Hox Associated Genes | Hox Signaling | -- |
| | | | | | |
| **sppa pathway** | Michigan | 18 | Signaling Pathway in Platelet Activation | Platelet Activation | -- |
| | | | | | |
| **Transport of vesicles** | Michigan,Boston | 17,17 | Vesicles Transport | Vesicles Transport | -- |
| | | | | | |
| **Hypoxia and p53 in the Cardiovascular system** | Boston | 1 | P53 Signaling in Hypoxia | Apoptosis | -- |
| **p53 signalling** | Michigan, Boston | 8, 12 | P53 Signaling | Apoptosis | -- |
| **Caspase pathway** | Stanford | 9 | Caspase Cascade | Apoptosis | -- |
| | | | | | |
| **Epithelial-mesenchymal transition (EMT)** | Boston | 14 | EM transition | Cell Migration/Metastesis | -- |
| | | | | | |
| **Mitochondrion (GO 0005739)** | Stanford | 18 | Mitochondrial | Cell Respiration | -- |
| **Mitochondrial genes** | Stanford | 11 | Mitochondrial | Cell Respiration | -- |
| **Human mitocondrial** | Stanford | 12 | Mitochondrial | Cell Respiration | -- |
| **Electron transport** | Stanford | 19 | electron transport | Cell Respiration | -- |
| | | | | | |
| **bcl2 family and reg. network** | Michigan | 15 | BCL2 Signaling | BCL2 Signaling | -- |

Table S6

| # probe set ids per gene | # genes | %genes |
|---|---|---|
| 1 | 10553 | 70.07 |
| 2 | 2758 | 18.31 |
| 3 | 1136 | 7.54 |
| 4 | 407 | 2.70 |
| 5 | 128 | 0.85 |
| 6 | 46 | 0.31 |
| 7 | 13 | 0.09 |
| 8 | 9 | 0.06 |
| 9 | 5 | 0.03 |
| 10 | 3 | 0.02 |
| 11 | 1 | 0.01 |
| 12 | 0 | 0.00 |
| 13 | 1 | 0.01 |
| Total | 15060 | |

**HGU133A**

| # probe set ids per gene | # genes | %genes |
|---|---|---|
| 1 | 8276 | 81.91 |
| 2 | 1326 | 13.12 |
| 3 | 381 | 3.77 |
| 4 | 83 | 0.82 |
| 5 | 18 | 0.18 |
| 6 | 11 | 0.11 |
| 7 | 6 | 0.06 |
| 8 | 3 | 0.03 |
| 9 | 0 | 0 |
| 10 | 0 | 0 |
| 11 | 0 | 0 |
| 12 | 0 | 0 |
| 13 | 0 | 0 |
| Total | 10104 | |

**HGU95AV2**

| # probe set ids per gene | # genes | %genes |
|---|---|---|
| 1 | 5670 | 89.8 |
| 2 | 516 | 8.17 |
| 3 | 102 | 1.62 |
| 4 | 18 | 0.29 |
| 5 | 2 | 0.03 |
| 6 | 4 | 0.06 |
| 7 | 1 | 0.02 |
| 8 | 1 | 0.02 |
| 9 | 0 | 0 |
| 10 | 0 | 0 |
| 11 | 0 | 0 |
| 12 | 0 | 0 |
| 13 | 0 | 0 |
| Total | 6314 | |

**HU6800**